Advanced Review

Enediynes, enyne-allenes, their reactions, and beyond

Elfi Kraka* and Dieter Cremer

Enediynes undergo a Bergman cyclization reaction to form the labile 1,4-didehydrobenzene (*p*-benzyne) biradical. The energetics of this reaction and the related Schreiner–Pascal reaction as well as that of the Myers–Saito and Schmittel reactions of enyne-allenes are discussed on the basis of a variety of quantum chemical and available experimental results. The computational investigation of enediynes has been beneficial for both experimentalists and theoreticians because it has led to new synthetic challenges and new computational methodologies. The accurate description of biradicals has been one of the results of this mutual fertilization. Other results have been the computer-assisted drug design of new antitumor antibiotics based on the biological activity of natural enediynes, the investigation of hetero- and metallo-enediynes, the use of enediynes in chemical synthesis and materials science, or an understanding of catalyzed enediyne reactions. © 2013 John Wiley & Sons, Ltd.

How to cite this article:
WIREs Comput Mol Sci 2013. doi: 10.1002/wcms.1174

INTRODUCTION

A review on the enediynes is necessarily an account of intense and successful interdisciplinary interactions of very different fields in chemistry involving among others organic chemistry, matrix isolation spectroscopy, quantum chemistry, biochemistry, natural product synthesis, drug design, medicinal chemistry, transition metal chemistry, or materials science. The roots of the enediyne chemistry can be found in a 1972 communication of Jones and Bergman in the *J. Am. Chem. Soc.*, in which the cyclization of (*Z*)-hex-3-ene-1,5-diyne (the parent enediyne of **1** in Figure 1) is described and evidence for the intermediate formation of the labile 1,4-didehydrobenzene (*p*-benzyne) provided (see **2** in Figure 1).[1] Already 1 year later, Bergman[2] published a review article on *Reactive 1,4-didehydroaromatics* because the work of the previous year related to the hot topics of the early 1970s: (i) the energetics of symmetry-allowed pericyclic reactions, (ii) aromaticity as a driving force for chemical reactions, and (iii) the investigation of labile intermediates with biradical character. The henceforth called Bergman cyclization provided deeper insight into the electronic structure of biradical intermediates, the mechanism of organic reactions, and orbital symmetry rules. Remarkable in this connection is that Bergman already derived in his review article reasonable energetics of the reaction on the basis of empirical considerations, decided for a biradical as the most likely electronic structure of *p*-benzyne (in view of the trapping products, which also confirmed its existence as an intermediate), and related the cyclization reaction to observations Masamune and co-workers[3] had made for cyclic enediynes also in the year 1972. These authors had obtained products that suggested the intermediacy of didehydronapthalene and 9,10-didehydroanthracene biradicals. In summary, several of the topics, which became relevant in enediyne research much later, are already contained in the 1973 review article of Bergman.[2]

Enediyne chemistry had a strong impact on a number of fields where quantum chemistry should be mentioned first. The *p*-benzyne was the first nontrivial biradical, for which, in view of the lack of experimental data, a reliable quantum chemical

The authors have declared no conflicts of interest in relation to this article.

*Correspondence to: ekraka@smu.edu

Computational and Theoretical Chemistry Group, Department of Chemistry, Southern Methodist University, Dallas, TX, USA

DOI: 10.1002/wcms.1174

 © 2013 John Wiley & Sons, Ltd.

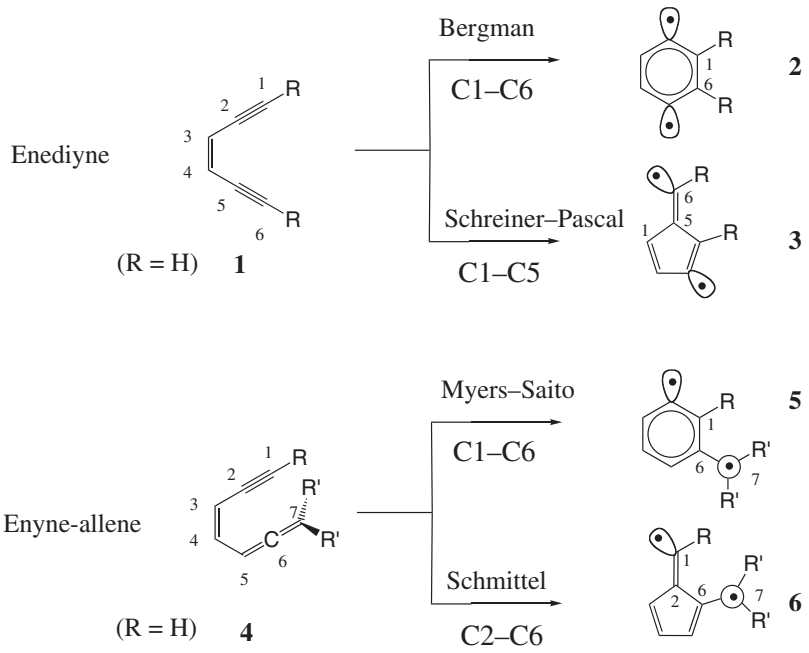

FIGURE 1 | Bergman, Schreiner–Pascal, Myers–Saito, and Schmittel reaction of enediynes and enyne-allenes.

description was needed. This need was enhanced by the discovery of natural enediynes in the 1980s.[4–6] The natural enediynes calicheamicin (1987),[5] esparamicin (1987),[6] and dynemicin (1990)[7] were soon after their discovery in the years 1987 and 1990 considered as possible leads for antitumor antibiotics where this hope was based on their relationship to neocarzinostatin.[8] The latter compound had already been discovered in 1965,[9] and its biological activity was early known. Neocarzinostatin can be considered as an enediyne with an epoxidized double bond, and therefore its biological activity was related to a Bergman-type cyclization of an intermediate enyne-cumulene.[10] Hence, the discovery of the natural enediynes and their chemistry established the importance of the cycloaromatization reaction discovered by Jones, Bergman, and Masamune in the early 1970s.

The Bergman reaction may be formally classified as an electrocyclic reaction.[11] However, it has to be mentioned that for an electrocyclic reaction, the 6π system orthogonal to the symmetry plane of **1** should be directly involved in the formation of the new CC bond, which is not the case. Other authors have related the Bergman reaction to the Cope rearrangement and speak of a *formal Cope rearrangement*.[12,13] Again, this can be questioned when considering just the Bergman reaction whereas the Bergman and retro-Bergman reaction seen together (i.e., considering both the formation of bond C1C6 to give **2** and the cleavage of bond C3C4 in **2**) may be formally seen in this way (interaction of two in-plane ally radicals) although this would lead to the transition state of the Cope rearrangement being identical to the intermediate *p*-benzyne biradical. In this situation, it is appropriate to follow the suggestion of Alabugin and coworkers[14] and to speak in the case of the Bergman and Myers–Saito rearrangements (Figure 1) of cycloaromatization reactions as a special class of ring-forming reactions.

The correct description of a singlet biradical such as *p*-benzyne requires a methodology, which was not available in the 1970s, however came into general use with the availability of coupled cluster methods[15] and perturbation theory corrected complete active space methods in the late 1980s and early 1990s, respectively.[16] A correct quantum chemical description of the Bergman cyclization implies more than just a reliable description of an organic biradical. It requires a balanced account of nondynamic (multireference) electron correlation effects (for the biradical) and dynamic electron correlation effects (especially including three-electron effects for the correct account of different types of electron delocalization in reactant and product). Even in the year 2013, this problem cannot be considered to be fully solved for the Bergman and the Bergman-related reactions (Figure 1) in the way that larger enediynes and enyne-allenes can be easily investigated.

In this situation, quantum chemists focused on the possibilities of density functional theory (DFT),[17]

 © 2013 John Wiley & Sons, Ltd.

which could be easily applied to larger systems and did not suffer as strongly as wave function theory from the basis set truncation error. It is fair to say that the study of enediynes and their reactions has led to a better understanding of DFT as well as to the development of new DFT methods with multireference character. Hence, a review on enediynes has to sketch the close connection between quantum chemical method development, especially in the 1990s and their application in the course of the investigation of enediyne reactions.

The possibility of using natural enediynes as antitumor antibiotics also triggered calculational studies especially in connection with computer-assisted drug design. These investigations were performed at a time when the medicinal work with natural enediynes had already suffered from setbacks due to their toxicity[8,18] so that after a period of heavy publication activity, editors had a tendency of "banning" enediyne articles from high-ranking journals. However, these setbacks opened up new perspectives rather than a decline of enediyne chemistry. The focus was now on nontoxic synthetic enediynes derived from their natural counterparts, the extension to hetero- and metallo-enediynes, the use of enediynes as polymers or other materials, and the application of Bergman-type reactions to discover new synthetic routes. Apart from this, it had already become a standard to test new quantum chemical methods for their accuracy by applying them to the benzyne biradicals and the cycloaromatization reactions of the enediynes and enyne-allenes. Hence, an enediyne review in the year 2013 is still carried by the fascination accompanying the natural enediynes as powerful anticancer drugs, the synthetic and mechanistic background of the enediyne reactions as well as the role, which enediyne chemistry still plays in quantum chemistry.

Previous reviews have focused on different aspects of enediyne chemistry including theory, thermodynamics and kinetics, vibrational spectroscopy, synthesis, biosynthesis, and pharmaceutical applications.

- *Theory*: The computational and theoretical background of enediynes was discussed by Schreiner and co-workers in 2005.[19] König and co-workers presented the electronic effects on the Bergman cyclization in 2004,[20] whereas Gilmore and Alabugin reviewed the enediyne chemistry in view of the Baldwin's rule for ring closure.[21] Two recently published reviews of Alabugin and co-workers discuss computational and theoretical studies of cycloaromatization reactions up to the year 2013.[14,22]
- *Thermodynamics and kinetics*: Wenthold provided an overview of all experimental thermochemical properties of benzynes up to 2010.[23] An earlier summary of benzyne chemistry complemented by a historic overview of their discovery and their applications in synthesis was given by Wentrup,[24] Recently, Schmittel et al. addressed the kinetics of the reaction bearing his name.[25]
- *Vibrational spectroscopy*: In 1998, Sander reviewed the vibrational spectroscopy of *m*- and *p*-benzyne.[26]
- *Photochemistry*: Recently, Alabugin and co-workers reviewed the photochemistry of enediynes.[27]
- *Synthesis*: The majority of recent reviews on enediynes give an overview over synthetic accomplishments. Joshi and Rawat published a comprehensive summary of the developments in enediyne chemistry.[28] Nicolaou and Chen reviewed the influence of enediynes on the development of total synthesis.[29] Maretina summarized design strategies of enediynes and enyne-allenes stretching from organic to metallorganic chemistry.[30] Guleskaya and Tyaglivy reviewed the use of enediynes in heterocyclic synthesis.[31]
- *Biosynthesis*: Liang highlighted the progress in the understanding of how natural enediynes are synthesized by nature.[32] Kar and Basak presented a comprehensive summary on the design of enediyne and related analogues with pH- or photodependent triggering devices.[33]
- *Pharmaceutical applications*: Shao reviewed the therapeutic applications of enediyne antitumor antibiotics,[34] and Popik summarized the efforts in the field of photoswitchable enediyne antibiotics.[35] Salas and co-workers published a summary on enediynes and related compounds produced from marine actinomycetes.[36]

This review will provide an overview of the past and current impact of enediynes in the field of computational chemistry. Special focus will be on the following topics: (i) the quantum chemical description of biradicals, (ii) the mechanistic studies of the Bergman cyclization and its related reactions, (iii) the computer-assisted design of target-specific enediyne antitumor drug candidates, (iv) enediynes as tools in syntheses, and (v) the role of enediynes in polymer chemistry and materials science.

© 2013 John Wiley & Sons, Ltd.

THE CHEMISTRY OF ENEDIYNES AND RELATED COMPOUNDS

In Figure 1, the prototypical cyclization reactions of enediynes and enyne-allenes are sketched. In addition to the Bergman cyclization, enediynes can also cyclize to a fulvene biradical **3** via a so-called Schreiner–Pascal cyclization first discussed in this connection by Schreiner.[37,38] Due to the lack of aromaticity and reduced conjugative stabilization of **3** as compared to **2**, this reaction can energetically not compete with the Bergman cyclization.[37] However, as shown in a recent experimental and theoretical study, the thermal cyclization can be enforced by steric hindrance at the alkyne termini.[38] Enyne-allenes **4** can perform the Myers–Saito[39,40] cyclization leading to the α-3-didehydrotoluene biradical **5**, whereas the corresponding Schmittel cyclization[41] generates the fulvene biradical **6**. There have been several reviews, which summarize the experimental investigations of these reactions,[23–25] and therefore only some of the highlights in the research on enediyne reactions are pointed out here, especially those, which turned out to provide reference data for the quantum chemical investigations on enediynes and their rearrangement products.

The Bergman Cyclization

Bergman[1,2] demonstrated that the reaction of the parent enediyne **1** is endothermic, has a significant barrier, and occurs only at temperatures higher than 155°C. In view of this limitation, the importance of this reaction in nature was not clear in the 1970s. This changed however dramatically in the mid-1980s. The discovery of the naturally occurring enediynes,[4–6,8,18] which perform a Bergman reaction to transform into biological active biradicals under physiological conditions, e.g., body temperature and a pH value close to 7, triggered a new wave of studies of this unique reaction. There was the expectation that understanding and copying what nature does could lead to new applications in the field of drug development.

In 1994, Rothet al.[42] determined the energetics of the Bergman cyclization of **1** with the help of kinetic measurements. They obtained a reaction enthalpy $\Delta\Delta H_0^f$ of 8.5 ± 1.0 kcal/mol. The activation enthalpies $\Delta H^{\ddagger}(\mathbf{1}-\mathbf{2},\ 470)$ and $\Delta H^{\ddagger}(\mathbf{2}-\mathbf{1},\ 470)$ for forward and backward reaction (see Figure 2), measured at 470 K, were 28.5 ± 0.5 and 19.7 ± 0.7 kcal/mol, which converts to values of $\Delta H^{\ddagger}(\mathbf{1}-\mathbf{2},\ 298) = 28.7 \pm 0.5$ kcal/mol and $\Delta H^{\ddagger}(\mathbf{2}-\mathbf{1},\ 298) = 20.2 \pm 0.7$ kcal/mol (see Figure 2) according to temperature corrections determined by Kraka and co-workers with the help of vibrational frequency calculations.[43] The relevant energy values are shown in Figure 2, where the activation enthalpy for the retro-Bergman cyclization is also given because this plays an important role for substituted enediynes as will be shown in the section on natural enediynes and the development of antitumor antibiotics. Noteworthy in this connection is that the energetics of the Bergman cylization as measured by Roth and co-workers[42] differed not much from the empirical estimates of Bergman in the early 1970s (32 and 18 kcal/mol for the activation enthalpies; 14 kcal/mol for the reaction enthalpy[2]).

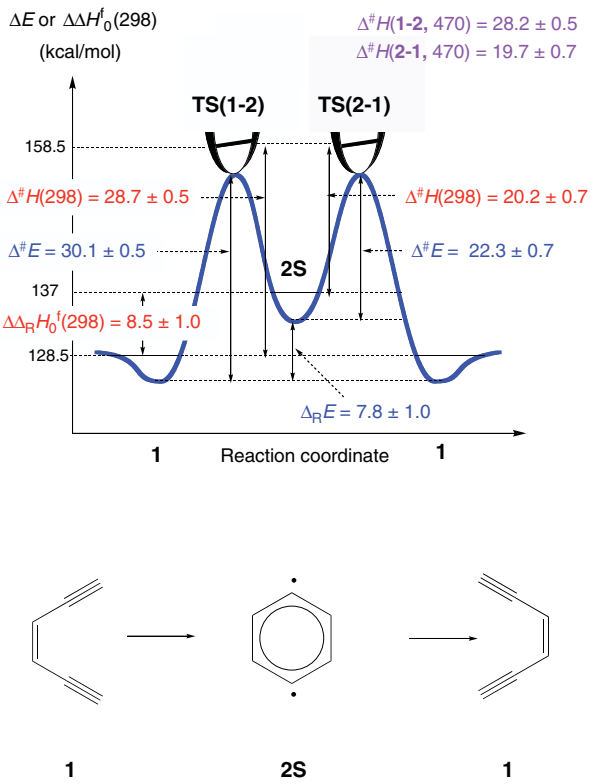

FIGURE 2 | Energetics of the Bergman cyclization of (*Z*)-hex-3-ene-1,5-diyne **1** as determined by experiment.[42] The experimental reaction enthalpy $\Delta\Delta H_0^f(298)$, the activation enthalpies for forward and backward reaction, $\Delta H^{\#}(\mathbf{1}-\mathbf{2},\ 470)$ and $\Delta H^{\#}(\mathbf{2}-\mathbf{1},\ 470)$, respectively, are converted to both enthalpy differences at 298 K and energy differences at 0 K ($\Delta_R E$, $\Delta E^{\#}(\mathbf{1}-\mathbf{2})$, $\Delta E^{\#}(\mathbf{2}-\mathbf{1})$) using vibrational corrections calculated at the B3LYP/6-311+G(3df,3pd) level of theory. (Reproduced with permission from Ref 43. Copyright 2000, American Chemical Society.)

Energy-resolved collision-induced dissociation (CID) measurements of Wenthold, Squires, and Lineberger (WSL)[44] determined the heats-of-formation of **2** to be 137.8 ± 2.9 kcal/mol. Combining Roth and co-workers' reaction enthalpy with the heats of formation for **1**, 105.0 kcal/mol,

© 2013 John Wiley & Sons, Ltd.

a heats-of-formation value of 138.0 ± 1.0 kcal/mol for **2** results, which is in convincing agreement with the CID measurements. Biradical **2** was isolated for the first time at low temperature in the matrix and identified by infrared measurements in combination with quantum chemical calculations by the Sander group and Kraka and Cremer.[45] These authors repeated in this way what they had already accomplished when identifying *m*-benzyne by matrix isolation spectroscopy for the first time.[46,47] The ground state of biradical **2** was proven to be a singlet in agreement with early predictions of Bergman and in line with what had been found for *m*-benzyne. WSL[44] reported a singlet-triplet splitting of 3.8 ± 0.4 kcal/mol for **2** where their measurements were based on the photoelectron-spectroscopy of biradical **2** and its anion. A recent comparison of the thermochemical properties of **2** with those of ortho- and meta-benzyne was published by Wenthold.[23]

The geometry of the parent enediyne **1** was investigated with the help of microwave spectroscopy by McMahon and co-workers.[48] The authors obtained an r_0 and r_s-structure from which an r_e geometry was derived with the help of CCSD(T) calculations. The latter geometry is in good agreement with high level *ab initio* calculations and confirms that the alkyne units are slightly bend outward leading to a critical distance C1C6 of 4.32 Å, slightly shorter than most DFT and early CCSD(T) calculations predicted. The CCC angles, indirectly responsible for this distance, turned out to be 123.9°.[48]

In contrast to the Bergman cyclization of **1**, the Myers–Saito cyclization of (*Z*)-1,2,4-heptatriene-6-yne **4** to the α-3-didehydrotoluene biracial **5** occurs at physiological conditions. The estimated activation enthalpy $\Delta H^{\ddagger}(\mathbf{4}-\mathbf{5})$ is 21.8 ± 0.5 kcal/mol. The reaction is exothermic with a reaction enthalpy $\Delta_R H =$ –15 ± 3 kcal/mol.[49] Recent multireference-MP2 calculations of Sakai and Nishitani[50] predict a $\Delta H^{\ddagger}(\mathbf{4}-\mathbf{5})$ of 16.9 kcal/mol and a $\Delta_R H$ of –14.0 kcal/mol thus confirming the experimental reaction enthalpy, however raising a question about the barrier height. For the Schmittel cyclization of **5**, Sakai and Nishitani[50] calculated a $\Delta H^{\ddagger}(\mathbf{4}-\mathbf{6})$ value of 22.9 kcal/mol and a $\Delta_R H = 10.5$ kcal/mol. No experimental data for the Schmittel reaction of **4** has been reported so far.

Controlling the Bergman Cyclization

The naturally occurring enediynes have inspired chemists to make strategical use of the Bergman cyclization in synthesis where these applications ranged from the natural product synthesis of target enediynes with antibiotic, antitumor activity to the use of designer enediynes in heterocyclic synthesis, polymer chemistry, and materials science.[21,28,30,31,51] For these purposes, the understanding of the kinetics of the Bergman cyclization and the electronic factors, which determine its barrier and the endothermicity of the reaction, is of fundamental importance. The barrier of the Bergman cyclization is influenced by three dominant factors: (i) the *proximity effect* first introduced by Nicolaou et a.[52]; (ii) the *molecular-strain differences* first discussed by Magnus et al.[53] and Snyder[54]; and (iii) the *electronic effects* influencing the stability of the rearranging enediyne, the corresponding transition state, or the formed biradical.

Proximity Effect

Nicolaou and co-workers[52,55] derived an empirical rule stating that the critical distance *R*(C1C6) between the two enediyne carbon atoms forming the new bond (see Figure 3) should be in the range of 3.31–3.20 Å for a spontaneous Bergman cyclization at body temperature (*proximity rule*). This rule has been confirmed and fine-tuned by quantum chemical calculations.[19,56] Noteworthy in this connection is that at a distance of 3.2 Å the two in-plane enediyne π-orbitals are parallel and resemble the orbital arrangement for the symmetry-forbidden transition state of the [2+2] cycloaddition reaction.[57] Alabugin and Manoharan point out that at this distance the four-electron repulsive interactions dominate the two-electron bond forming interactions according to an natural bond orbital (NBO) analysis.[57] At a distance below 3.2 Å, the two-electron stabilization interactions steeply increase thus supporting bond formation.

As Figure 3 reveals, the parent enediyne has a large barrier because of a C1C6 distance of 4.41 Å. This distance can be stepwise reduced by incorporating the enediyne unit into 12- or 10-membered rings where benzoannelation and the incorporation of heteroatoms or sp^2-hybridized C atoms (double bonds) leads to a further decrease of the critical distance. A spontaneous Bergman reaction is found for benzodecapentaene below 25°C in line with a critical distance of just 3.01 Å.[58] Figure 3 reveals that not all activation enthalpies follow the proximity rule and that other factors also influence the reactivity of the enediyne.

Nevertheless, the proximity rule helps to understand the reactivity of some natural enediynes, which must be appropriately triggered to become bioactive. For example, dynemicin (see Figure 4) contains in its untriggered form an epoxide that locks the 10-membered enediyne ring in a conformation that

 © 2013 John Wiley & Sons, Ltd.

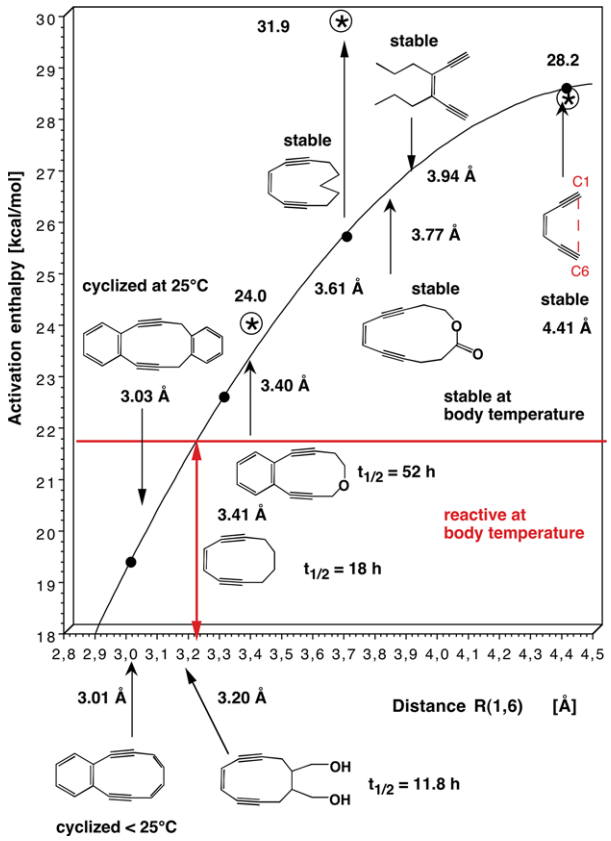

FIGURE 3 | Dependence of the activation enthalpy of the Bergman cyclization of (Z)-hex-3-ene-1,5-diyne on the critical distance between carbon atoms C1 and C6 according to *ab initio* calculations (black dots).[56] Known C1C6 distances, measured activation enthalpies (starred values), half-life times $t_{1/2}$, and cyclization temperatures are also given.[55] The deviations of the starred values indicate the limitations of the *ab initio* relationship. (Reproduced with permission from Ref 56. Copyright 1994, American Chemical Society.)

freezes the critical distance at 3.54 Å.[59] Triggering of dynemicin opens the epoxide ring, changes the conformation of the 10-membered ring, and decreases the critical distance to 3.17 Å. Consequently, the barrier for the Bergman cyclization is lowered from 52 to 17.9 kcal/mol.[59]

Molecular-Strain Differences

Despite a large body of theoretical and experimental evidence supporting the proximity rule, Magnus et al.[53] and Snyder[54] proposed that the driving factor for the Bergman reaction is the difference in strain energies for the ground and transition state of the enediyne. An early study by Magnus and coworkers[53] showed that the [7.3.1] bridgehead ketone **7** (see Figure 5) performs the Bergman cyclization already at 70°C whereas the [7.2.1] bridgehead ketone **8**, which possesses a decreased critical distance of 3.36 Å, reacts about 660 times slower than **7**. The authors explained the unexpected reactivity by pointing out that in **7** the six-membered ring converts from a boat conformation in the starting situation to a chair conformation in the transition state thus reducing its strain energy by about 6 kcal/mol, which lowers its activation energy from 31.2 in **8** to 25.4 kcal/mol in **7**.

In a recent study, Basak and co-workers[60] compared the cyclization rates of two enediynes with the same critical distance (3.79 Å) but different degrees of saturation in a heterocyclic chromophore linked to the enediyne unit (see **9–12** in Figure 5). Compound **9** contains an aromatic 6π ring, which forces the heavy atoms of the $-O-CH_2$ substituent into the ring plane thus leading to a highly strained eight-membered ring in the transition state **10** of the cyclization. Saturation of the remote double bond in the diaza-cyclohexenone ring of **11** results in a strain relief of the eight-membered ring, which is due to the higher flexibility of the diaza-cyclohexenone unit.

These examples clearly emphasize the general importance of ring strain in the enediyne and related cyclizations. Strain in the starting enediyne will raise its energy, which, with increasing cycloaromatization, will be lowered in the transition state. The proximity rule is a simple measure of this strain, however cannot account for other strain effects resulting from bicyclic structures. Hence, the proximity rule applies only to simple enediyne situations, whereas more complex structures require a detailed strain analysis. All naturally occurring enediynes are incorporated into 9- or 10-membered rings, which increases the strain of the reactant in the sense of the proximity rule. This explains the exclusive focus on the critical distance by those who were involved in the synthesis of natural enediynes.[61–63]

In a recent review article, Alabugin and coworkers[14] give an appealing analysis of strain effects. They emphasize that strain can act in two different ways, which they discuss for enediynes as follows: Strain induced at the ene unit (incorporation of the double bond in a strained ring) lowers the reactivity of the reactants and accordingly is unproductive, whereas strain induced at the alkyne termini, e.g., by incorporating them in a strained ring, facilitates cycloaromatization and therefore is productive.[14]

Electronic Effects

Much effort has been invested into the unraveling of the electronic effects influencing the energetics of the Bergman cyclization.[19,20,64,65] These effects may be distinguished in the following way: (i) influence of substituents at the terminal alkyne positions,

 © 2013 John Wiley & Sons, Ltd.

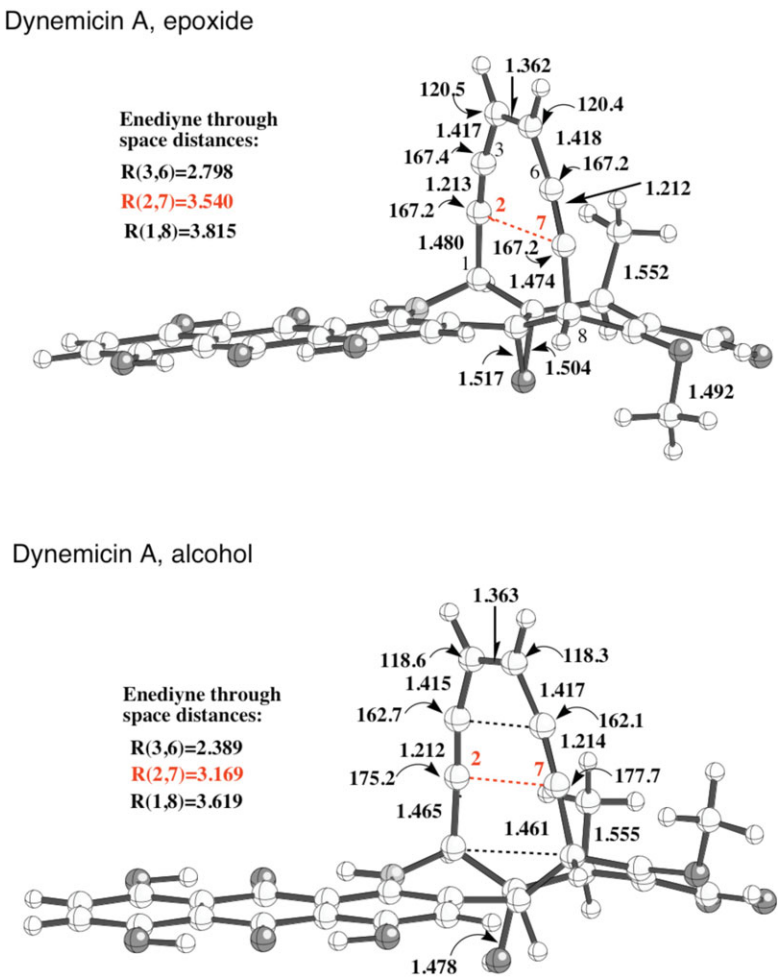

FIGURE 4 | Change in the critical distance C2, C7 (corresponding to C1, C6 in **1**) before and after opening of the epoxide in dynemicin A.[59]

(ii) influence of substituents at the vinyl positions, (iii) benzannelation, and (iv) extension of (iii) to the so-called *ortho-effect* of o-positioned benzo-substituents.[66]

(i) Terminal substitution. Substituents with σ-withdrawing and π-donating capacity such as –F, –Cl, –OH, NH_3^+ decrease the barrier and endothermicity of the Bergman cyclization whereas σ-donating and π-withdrawing substituents such as $-BH_2$, $-AlH_2$ produce the reverse effect.[65] In the case of substituents with both σ- and π-withdrawing effect such as $-NO_2$, the σ-withdrawing influence dominates.

In Figure 6(a), the highest occupied π- and σ-orbitals of *p*-benzyne are shown where the nodal planes are indicated by dashed lines. There is another π-orbital close, but lower in energy and with a horizontal nodal plane, which leads to less exchange repulsion between the X orbitals. Also, it has to be mentioned that the C2, C5 coefficients of the π-orbital considered may have positive, negative, or zero value depending on the electronic nature of X. Normally, the σ-HOMO (highest occupied molecular orbital) is above the πHOMO (actually the HOMO-1); however, this will depend on X.

Substituents with π-donor character will increase the density between atoms C1 and C6 in the π-HOMO, thereby facilitating bond formation between these atoms, which leads to a lowering of the reaction barrier. Substituents with σ-withdrawing character will decrease the electron density in the σ-HOMO, which is C1C6 antibonding (Figure 6(a)). This again will lead to a stabilization of the transition state and, hence, a lowering of the barrier. Even remote substituents at the alkyne terminus can influence the cyclization mechanism, forcing it from a concerted to a stepwise mechanism as was recently shown by Schmittel and co-workers.[25,67]

(ii) Vinyl substitution. It has been found that electron-withdrawing groups such as NO_2 or OH in a vinyl position increase the barrier of the Bergman

 © 2013 John Wiley & Sons, Ltd.

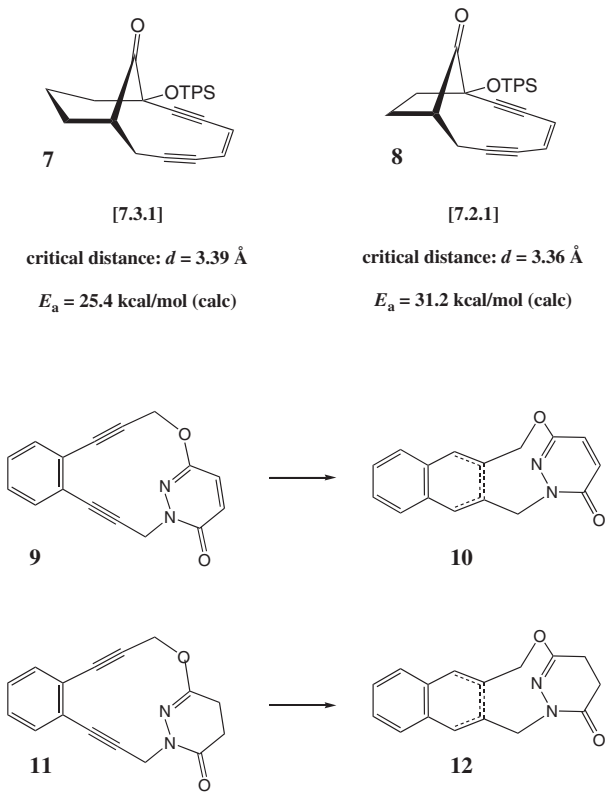

FIGURE 5 | Influence of strain effects on the barrier of the Bergman cyclization.

cyclization. σ-Donating groups lower the barrier, whereas π-donation has only a minor effect.[64] It was argued that the transition state is "σ-aromatic" and accordingly stabilized by σ-donating groups; however, no arguments were given why σ-aromaticity is in this case stronger than π-aromaticity.[19] Similarly, one has referred to the nature of the HOMOs shown in Figure 6(a) without providing a consistent explanation of the role of vinyl substituents. An improved discussion of the situation was given by Alabugin and Manoharan.[68]

Special consideration was given to the effect of halogens in vinyl positions, which are known to increase the barrier of the cycloaromatization reaction. Jones and co-workers[69,70] invoked increasing exchange repulsion between the in-plane Cl electron lone-pair and the in-plane π-electrons, which were assumed to increase in the course of the reaction. No details were given. The situation is sketched in Figure 6(b). Repulsion between the electrons of the orbitals shown will be determined by geometric and hybridization factors. Clearly, the geometric factors are as such that repulsion should decrease rather than increase with the bending at C2. However, the bending involves also a rehybridization of a $p\pi$- to a sp^2-orbital, which extends much more into space and therefore overlaps more strongly with the in-plane lone pair orbital at Cl. It seems that the latter effect dominates, thus causing an increase in the barrier as caused by the Cl substituents.

(iii) Benzoannelation. Replacing the enediyne double bond by a benzene ring leads to a special form of vinyl substitution. Under comparable conditions, Roth and co-workers[71] found that for 1,2-diethynylbenzene (see Figure 6(c)) the energetics of the Bergman cyclization significantly changes as is reflected by a 3 kcal/mol decrease in the barrier (decrease from 28.2 kcal/mol in the case of **1** to 25.2 kcal/mol) and a large increase of the endothermicity by 9.4 kcal/mol (from 8.5 to 17.5 kcal/mol). Since benzoannelation reduces the C1C6 distance by more than 0.3 Å, the decrease in the barrier is not unexpected.

The increased endothermicity was attributed to a reduced gain in aromatic stabilization when transforming 1,2-diethynylbenzene to 1,4-didehydronaphthalene **14**compared to the aromaticity gain for the parent enediyne **1**. Benzo-annelation reduces the barrier of the retro-Bergman ring-opening reaction to 7.7 kcal/mol (Figure 6(c)) and makes the hydrogen atom abstraction the rate-determining step. A recent study on aryl-fused quinoxalenediynes[72] concluded that extending benzoannelation from 1,2-diethynylbenzene in a linear fashion with respect to the enediyne core further increases endothermicity of the Bergman cyclization, whereas extending benzoannelation in an angular orientation (starting with **13** as the parent system) leads to the opposite effects. These trends can be summarized by Clar's rule according to which arenediynes that produce new aromatic sextets lead to more favorable Bergman cyclization products due to increased aromatic stabilization.

(iv) Ortho-effect Alabugin and co-workers[66,73,74] showed that ortho-substitution in benzoannulated enediynes significantly influences the Bergman cyclization via a combination of electronic, steric, and electrostatic effects involving the in-plane orbitals. Electron-acceptor substituents are generally found to accelerate the cyclization because electron repulsion between the occupied in-plane alkyne π-orbitals is reduced in the course of the reaction. However, this can be overruled by steric factors or hydrogen bonding. *Syn*-CHO, *ortho*-NO_2, CF_3, and *syn*-OMe_3 facilitate the Bergman cyclization through steric assistance forcing the alkyne groups to bend. Steric repulsion in the reactant is alleviated in the transition state where the acetylene moiety is bent away from the ortho substituent. CH_3, NH_2, and *syn*-OH increase the activation energy

 © 2013 John Wiley & Sons, Ltd.

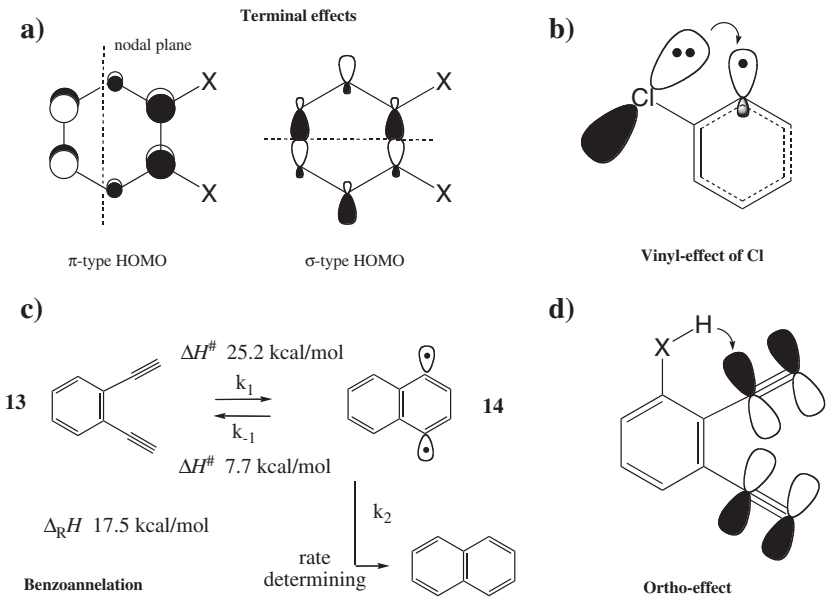

FIGURE 6 | Electronic effects determining the energetics of the Bergman cyclization (see the text).

because they stabilize the starting material by a hydrogen bond between XH and the in-plane alkyne π-orbital (Figure 6(d)). As the reaction proceeds, this stabilizing interaction disappears and is replaced by a H-bond to a radical center. This can lead to an internal H-abstraction reaction and the formation of an oxyl radical.

Acyclic Enediynes

New synthetic results in enediyne chemistry have revealed that acyclic enediynes can be thermally stable and nevertheless undergo the Bergman cyclization at body temperature. In these cases, special electronic effects stabilize the cyclization product, which we will discuss for some examples shown in Figure 7. (For a more comprehensive review, see Ref. 28.)

Lin and co-workers[75] synthesized acyclic enediynes with aromatic N-heterocycles in the terminal position of the alkyne. Compounds such as **15** and **16** (X = CH, N) showed growth inhibition effects for X = N on a full panel of 60 human cancer cell lines. The biradicals of **15** and **16** formed during the Bergman cyclization are stabilized by electrostatic

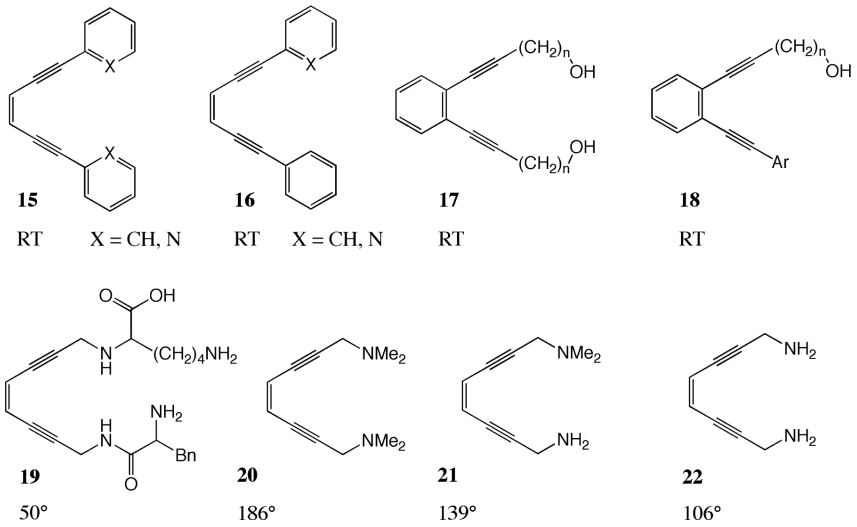

FIGURE 7 | Acyclic enediynes undergoing the Bergman cyclization at either room temperature (RT) or reduced temperature. Temperatures are in °C are given below formulas.

© 2013 John Wiley & Sons, Ltd.

interactions between the two heterocycles, which are free to rotate into a position maximizing intramolecular dipole–dipole attraction. Lo and coworkers[76] introduced enediynes **17** and **18**, which possess (a) terminal OH group(s) and potent anticancer activity. In these cases, the biradicals are stabilized by hydrogen bonding. Compound **18** displayed a broad spectrum of inhibition for various cancer cell lines. The authors argued that the arene substituent at the terminal alkyne position is needed to obtain antiproliferation.

Jeric and co-workers[77,78] introduced a general strategy for the preparation of enediyne–amino acid conjugates such as **19**. Their study showed that peptide-based enediynes can undergo Bergman cyclization at relative low temperatures where H-bonding between the terminal groups may play a role. Rawat and Zaleski[79] investigated the influence of bulky substituents at the alkyne termini of N-substituted enediynes. The barrier for the Bergman cyclization is lowered by 80°C when replacing the bulky NMe_2 substituents in **20** by NH_2 stepwise via **21** to **22** (Figure 7). Compound **22** may turn out to be an important ligand for the synthesis of thermally reactive metallo-enediyne complexes. The Bergman cyclization barriers of diethynyl-imdidazole derivatives can be modulated by suitable N-substituents.[80] In this way, they offer a promising potential for drug design.

COMPUTATIONAL DESCRIPTION OF ENEDIYNES AND THEIR REARRANGEMENT PRODUCTS

The quantum chemical description of enediynes and their reactions is challenged by the fact that in the Bergman, Myers–Saito, or Schmittel reaction always a closed-shell system (the enediyne) rearranges to an open-shell singlet biradical with substantial multireference character. This requires methods, which provide a balanced description of both reactant and product in addition to a cost-effective handling of large molecular systems (Figure 1; R being a bulky group). Because these two requirements were (are) difficult to fulfill, quantum chemists focused in the beginning (i) on the computational investigation of the parent enediyne or enyne-allene system shown in Figure 1 and (ii) on the extensive use of DFT.

DFT Description of Bergman and Related Reactions

Kohn–Sham DFT (KS-DFT) is a single-determinantal method that can in principle describe multireference systems provided the exact exchange-correlation (XC) functional would be known.[17] However, with the approximate XC functionals nowadays available a restricted DFT (RDFT) description of the Bergman, Schmittel, or Myers–Saito reaction has to fail because of an erroneous description of biradicals **2**, **3**, **5**, and **6** (Figure 1) formed in these reactions. In view of the size of the naturally occurring enediynes, there was (and still is) the dilemma of using a low-cost method such as DFT, but having to describe transition states and products with considerable biradical character. This dilemma motivated the analysis of existing and new DFT methods, which centered around broken-symmetry spin-unrestricted DFT (BS-UDFT),[43,81] permuted orbital UDFT (PO-UDFT),[81] two-determinant DFT methods such as ROSS (restricted open-shell-singlet)-DFT,[82] ROKS (restricted open-shell Kohn–Sham) DFT,[83] and REKS (restricted ensemble Kohn–Sham) DFT[84,85] as well as the complete active space DFT (CAS-DFT) method.[86–88] For each of these methods, the choice of the X and/or C functional turns out to be decisive.

Early success in describing open-shell singlet (OSS) biradicals with UDFT caused many authors to use DFT in situations where this method should fail for principle reasons. This led to a dispute between DFT developers and DFT users where especially enediyne chemistry was the battlefield of contradictory opinions. Scientific disputes tremendously help to clarify methodological questions where in the case of the enediynes the problems concerning the reasonable description of σ,σ- and σ,π-OSS biradicals were solved.

Electron Correlation Effects Relevant in Enediyne-Related Molecules

In Figure 8, four adiabatic connection schemes[81] are given, which schematically describe the electron interaction systems related to enediynes. For $\lambda = 0$, the reference state with noninteracting electrons is defined, which, by increasing λ from 0 to 1, is adiabatically converted into a system with real electron–electron interactions. In the way λ increases, dynamic electron correlation will increase from zero to its full magnitude (correlation energy E_C in Figure 8) and a continuum of intermediate states will connect the reference to the real state of the electronic systems given at the bottom of Figure 8.

As a closed-shell system, an enediyne can be presented in its ground state by one configuration state function (CSF) Ψ_0, which in turn can be approximated by one Slater determinant Φ_0, i.e. the ground state of an enediyne can be reasonably described by a single-configurational, single-determinantal wave function. In Figure 8, this is called a type 0 system, which can be satisfactorily described by KS-DFT.

 © 2013 John Wiley & Sons, Ltd.

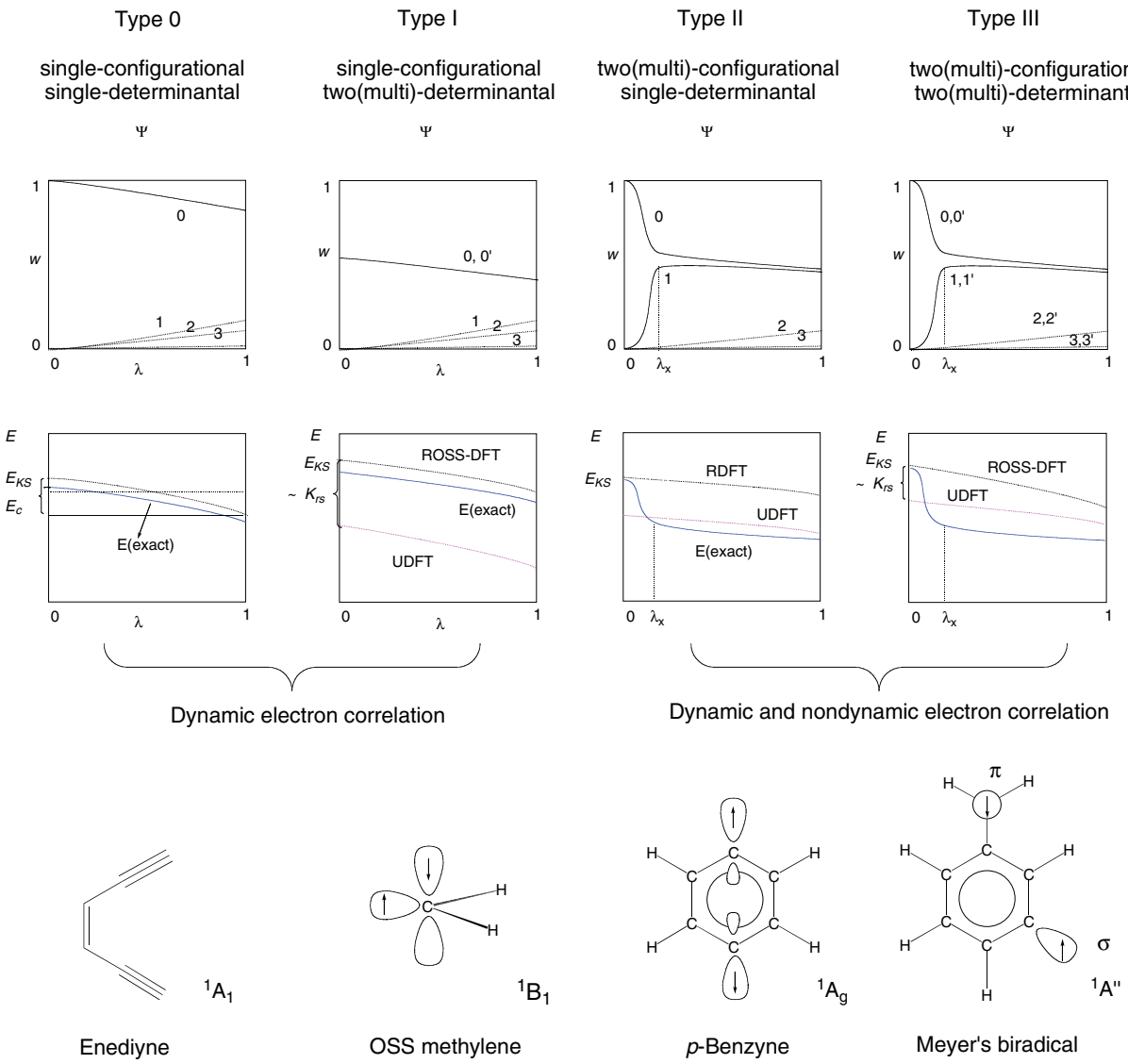

FIGURE 8 | Schematic representation of wave function and energy of type 0, type I, type II, and type III electronic systems as described by RDFT or UDFT with approximate exchange-correlation functionals (dotted lines) or exact Kohn–Sham DFT (solid line).[81] Numbers 0, 1, 2, etc. denote CSF Ψ_0, Ψ_1, Ψ_2, etc. or determinants Φ_0, Φ_1, etc. The weights w of the CSF in the true wave function are schematically shown (first row of diagrams) in dependence of the parameter λ that stepwise increases the electron correlation energy E_c from zero ($\lambda = 0$) to its true value ($\lambda = 1$). The corresponding changes in the Kohn–Sham energy E_{KS} and in the exact energy E(exact) (blue) are schematically given in the second row of diagrams. For each type of electronic system, a molecular representative is given at the bottom where one of several electron configurations is indicated. (Reproduced from Ref 81. Copyright 2002, MDPI.)

Excited determinants Φ_1, Φ_2, etc. (described also as $\Phi_{ijk\ldots}^{abc\cdots}$, where $i, j, k, \ldots$ denote the indices of occupied orbitals, from which electrons have been excited to virtual orbitals $a, b, c, \ldots$) are required in a wave function expansion to describe dynamic electron correlation effects, which are essential for conjugated systems such as the enediynes. This however does not exclude that Φ_0 still dominates the wave function and that these correlation contributions can be assessed by the correlation functional of DFT leading to the correlation correction E_C.[81,89]

In the transition state region of the enediyne cyclization reaction, the reactant adopts biradicaloid character. Two different situations emerge depending on whether a Bergman or Schreiner—Pascal reaction (Myers–Saito or Schmittel in case of an enyne-allene) takes place. In the first case, the closed-shell system of the reactant is gradually converted into the open-shell singlet biradical *p*-benzyne that can be essentially

 © 2013 John Wiley & Sons, Ltd.

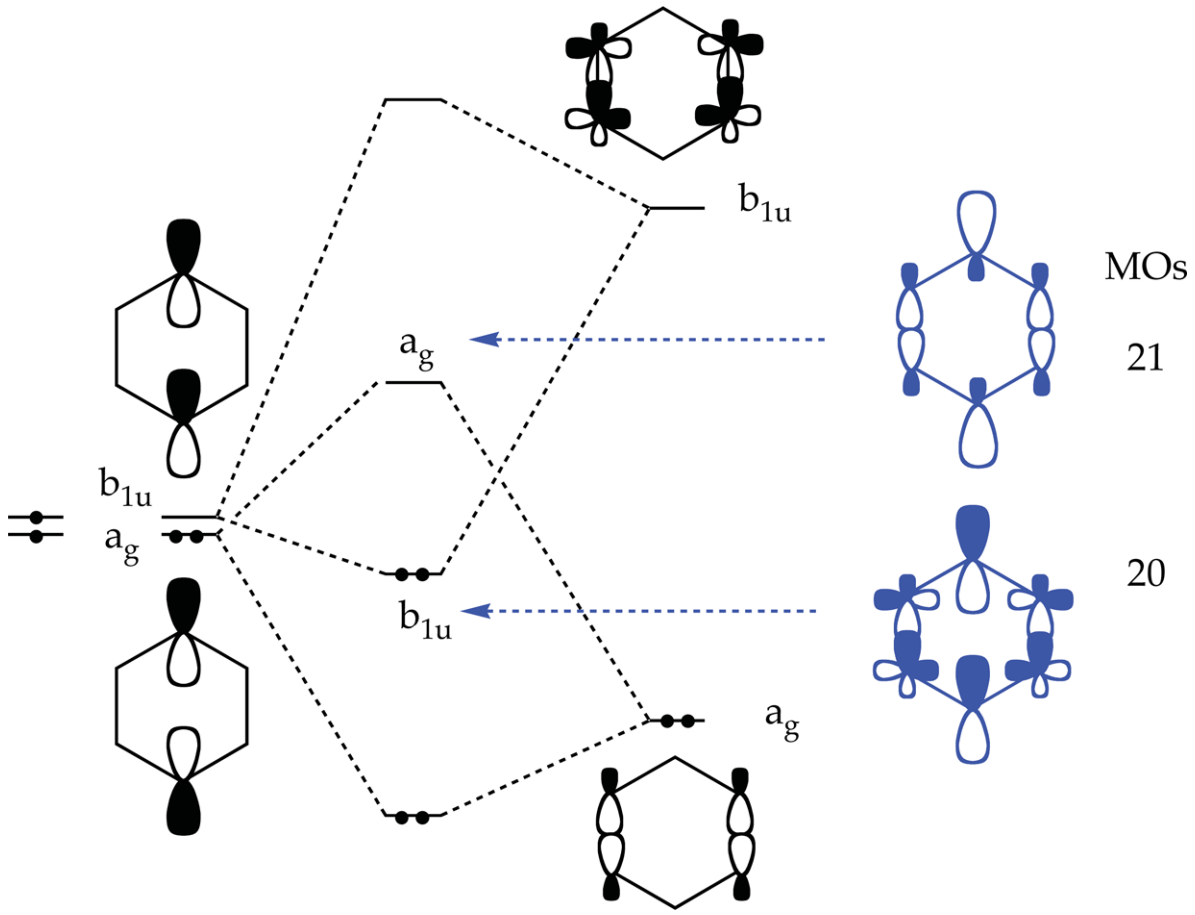

FIGURE 9 | Frontier orbitals of *p*-benzyne (in blue), which result from through-bond interactions involving the singly-occupied orbitals (on the left) and the $\sigma(C2C3;C5C6)/\sigma^*(C2C3;C5C6)$ orbitals (on the right).

described by a two-configurational approach in its S_0 ground state where each configuration is given by a single Slater determinant. This corresponds to a type II system in Figure 8. The dominating two Slater determinants for *p*-benzyne are (compare with Figure 9):

$$\Phi_0 : \cdots (1b_{3u})^2(1b_{2g})^2(1b_{1g})^2(5b_{1u})^2(6a_g)^0$$
$$\Phi_1 = \Phi_{ii}^{aa} : \cdots (1b_{3u})^2(1b_{2g})^2(1b_{1g})^2(5b_{1u})^0(6a_g)^2$$

The coefficients of these two Slater determinants reflect the biradical character of *p*-benzyne. The latter successively grows from the transition state to the product where it would be 100% if orbitals $5b_{1u}$ and $6a_g$ would be truly degenerate (see Figure 9). However, the latter can interact with the a_g-symmetrical $\sigma(C2C3;C4C5)$ and b_{1u}-symmetrical $\sigma^*(C2C3;C4C5)$ orbitals. This leads to *through-bond electron delocalization* of the single electrons and a lowering of the energies of HOMO and HOMO-1 as shown in Figure 9. The biradical character of *p*-benzyne is reduced in the way the molecule is stabilized. However, there is no experiment, which can conclusively determine either the degree of stabilization or the degree of biradical character. This can only be assessed by quantum chemical calculations where simplifications may lead to a bias toward too much or too little biradical character (see below). Again, this will depend on the amount of dynamic electron correlation included by a given method because the latter is also essential to describe through-bond electron delocalization correctly. In any case, *p*-benzyne is a two-configurational, two-determinantal problem (for each configuration only one determinant is needed), which is best described by a multireference method.

As shown for type II systems in Figure 8, the weight w_1 of the determinant Φ_1 strongly increases at some point λ_x so that the wave function is no longer dominated by Φ_0. The exact energy E(exact) drops at this point substantially below the KS energy thus underlining the importance of nondynamic electron correlation. Dynamic electron correlation effects are

 © 2013 John Wiley & Sons, Ltd.

accounted for by small, but significant contributions of excited determinants Φ_2, Φ_3, etc.

Multireference Effects Provided by RDFT

RDFT with approximate XC functionals often suffer from the self-interaction error (SIE).[90] In Hartree–Fock (HF) theory, the self-repulsion energy of an electron is exactly canceled by its self-exchange energy. In DFT, this is no longer the case because of the approximations made when setting up the X functional. Hence, a SIE (X-SIE) results, which can be substantial, especially in the case of odd-electron systems or charge transfer situations.[91] Also, a single electron does not possess any self-correlation energy. C functionals, which are based on wave function descriptions of the correlation hole such as the Lee Yang Parr (LYP) functional (derived from the Colle–Salvetti functional[92] do not suffer from a SIE (C-SIE); however, this may not be an advantage. Often the X-SIE and C-SIE have opposite signs and therefore cancel each other to some extentwhere the total SIE is always dominated by the X-SIE.[89]

Cremer and co-workers have investigated the exchange-hole (X-hole) as described by LDA (local density approximation) and GGA (generalized gradient approximation) functionals.[91–96] These authors showed that the error introduced by the local character of the LDA and GGA X-functionals mimics long-range, left-right correlation effects. This can be made visible by comparing exchange-only DFT electron density distributions directly with coupled cluster density distributions. Both types of densities reveal features that are strongly reminiscent of left-right correlation.[97]

The X-SIE leads to the improved performance of KS-DFT in the case of electronic systems with multireference effects. However, this fact must not be misunderstood as a guarantee that DFT with SIEs can correctly describe multireference systems. The inclusion of nondynamic electron correlation via the SIE of the X-functional is done in a nonspecific way and therefore cannot adjust to the situation of multireference systems with specific nondynamic electron correlation effects. If the SIE-induced correlation effects lead to an improvement of DFT results, it will certainly be for the wrong reason that provides an uncertain starting point for further method (or XC) developments in DFT. Noteworthy in this connection is the fact that hybrid functionals with an increasing portion of exact exchange suffer less from the X-SIE, however become also more unstable in the case of multireference systems. This has to be considered when describing enediyne or enyne-allen reactions with DFT.

An improvement of DFT in the way that multireference effects are explicitly included can lead to a deterioration of results on biradicals such as **2** or **3** compared to the use of XC-functionals with an SIE. This results often from a double counting of correlation effects (specific and nonspecific ones). In such cases, the performance can be improved when replacing GGA functionals such as BLYP with hybrid functionals such as B3LYP because the latter suppress the nonspecific multireference contributions brought about by the X-functional and its SIE. This has often been overlooked in the studies of enediyne reactions.

Broken Symmetry UDFT Description of p-Benzyne

Also shown in Figure 8 is the fact that UDFT can mimic the multireference character of type II systems under certain conditions. The UDFT wave function (abbreviated by U) is given as a product of a (closed-shell) core part Ψ_{core} and an open-shell part Ψ_{open}:

$$\Psi^{\text{U}} = \mathcal{A}\left\{\Psi^{\text{U}}_{\text{core}}\Psi^{\text{U}}_{\text{open}}\right\} \tag{1}$$

(where $\mathcal{A}$ is the antisymmetrizer; $\Psi^{\text{U}}_{\text{core}}$ will no longer represent an exact closed-shell function in the final unrestricted wave function due to the independent optimization of the α- and β-spin orbitals). In the case of *p*-benzyne, $\Psi^{\text{U}}_{\text{open}}$ is constructed from the b_{1u}-symmetrical HOMO and the a_g-symmetrical lowest unoccupied molecular orbital (LUMO) for the purpose of yielding a broken-symmetry UDFT (BS-UDFT) description of the ^1A_g state (Figure 8). This is achieved by mixing the HOMO and the LUMO of the closed shell RDFT description of the ^1A_g state.[43,81]

$$\Psi^{\text{BS-U}}_{\text{open}} = |\psi_r\overline{\psi_s}\rangle \tag{2}$$

where the bar denotes a β spin orbital, and the spin orbitals are given by

$$\begin{aligned}\psi_r &= \cos\theta\ \ \psi_{\text{HO}} + \sin\theta\ \ \psi_{\text{LU}}\\ \psi_s &= -\sin\theta\ \ \psi_{\text{HO}} + \cos\theta\ \ \psi_{\text{LU}}\end{aligned} \tag{3}$$

The orbital rotation angle θ is optimized during the self-consistent field (SCF) iterations. The resulting orbitals ψ_r and ψ_s are the localized counterparts of HOMO and LUMO, respectively (see Figure 10). Using Eq. (2), the open-shell part $\Psi^{\text{BS-U}}_{\text{open}}$ of the BS-UDFT wave function can be written in the form of Eq. (4).

$$\begin{aligned}\Psi^{\text{BS-U}}_{\text{open}} = \cos^2\theta\ \ |\psi_{\text{HO}}\overline{\psi_{\text{HO}}}\rangle - \sin^2\theta\ \ |\psi_{\text{LU}}\overline{\psi_{\text{LU}}}\rangle\\ + \sqrt{2}\cos\theta\sin\theta\ \ |\psi_{\text{HO}}\overline{\psi_{\text{LU}}}\rangle^T.\end{aligned} \tag{4}$$

© 2013 John Wiley & Sons, Ltd.

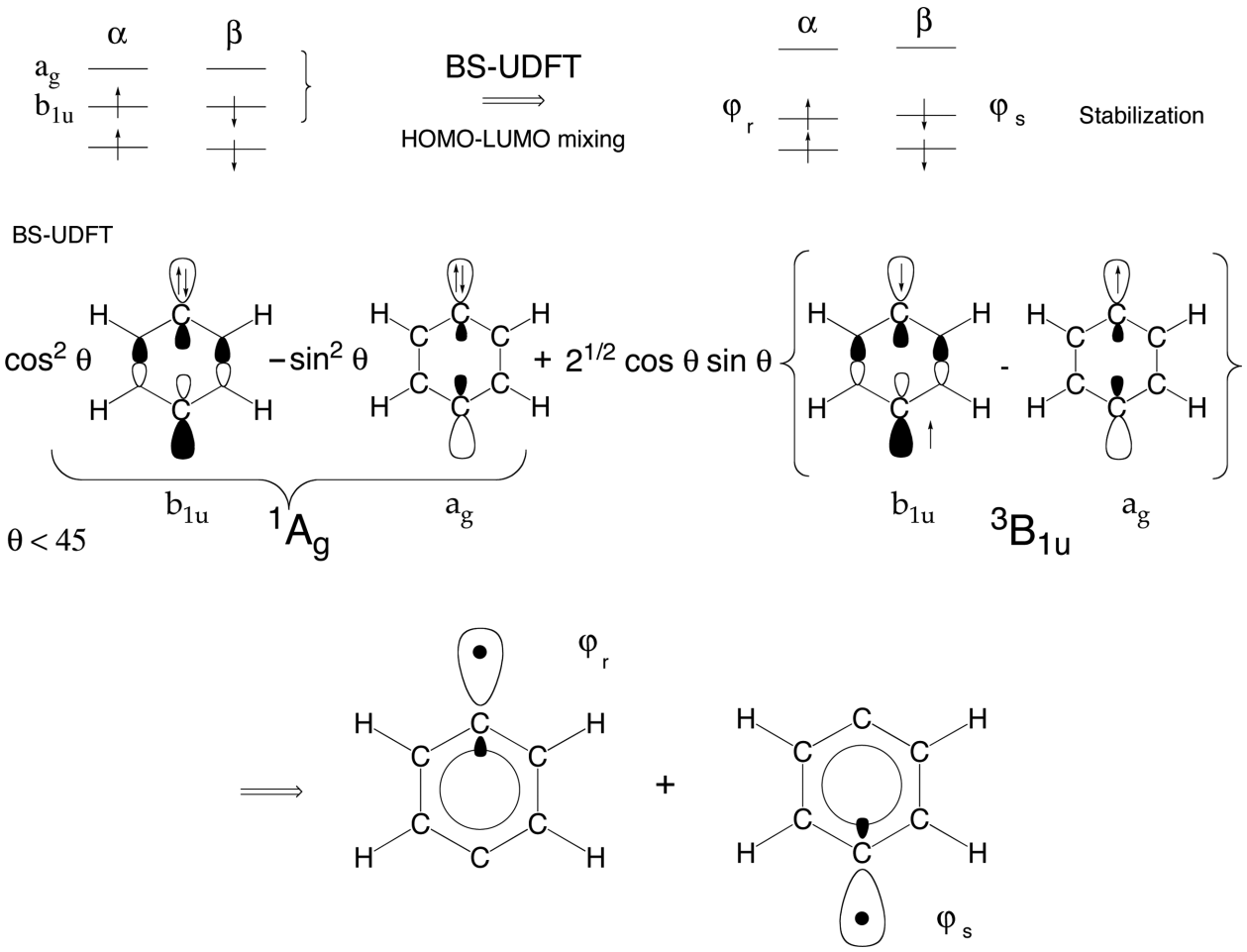

FIGURE 10 | Schematic representation of the ^1A_g state of *p*-benzyne by a BS-UDFT wave function. The HOMO–LUMO mixing is given schematically where the form of the frontier orbitals has been simplified to local orbitals φ_r and φ_s.

where HO and LU denote the HOMO and LUMO . A bar over the orbital symbol indicates β-spin, and the triplet function is given by

$$|\psi_{b_{1u}}\overline{\psi_{a_g}}\rangle^T = \frac{1}{\sqrt{2}}\left(|\psi_{b_{1u}}\overline{\psi_{a_g}}\rangle - |\psi_{a_g}\overline{\psi_{b_{1u}}}\rangle\right). \qquad (5)$$

Hence, the BS-UDFT state is a mixture of the $|\psi_{\mathrm{HO}}\overline{\psi_{\mathrm{HO}}}\rangle$ and $|\psi_{\mathrm{LU}}\overline{\psi_{\mathrm{LU}}}\rangle$ singlet states and the $|\psi_{\mathrm{HO}}\overline{\psi_{\mathrm{LU}}}\rangle^T$ ($M_S = 0$) triplet state. The spin symmetry is broken, and with respect to the spatial symmetry, the BS-UDFT reference state does not belong to any irreducible representation but is part of a reducible representation that consists of a ^1A_g and a $^3B_{1u}$ contribution for *p*-benzyne. However, the BS-UDFT reference function is not completely asymmetric: It belongs to an irreducible representation of a mixed spin-space symmetry group where all reflections at the mirror plane are combined with a simultaneous flip of all spins in the system.[81]

The BS-UDFT wave function has two-configurational character similar to that of the generalized valence bond approach for one electron pair (GVB(1)).[98] Hence, the BS-UDFT orbitals ψ_r and ψ_s resemble the corresponding GVB orbitals (see Figure 10). However, the BS-UDFT wave function does not adopt the two-configurational (two-determinantal) form given by the first two terms in Eq. (4) (ground state and doubly excited state) because the admixture of the triplet state function leads to a collapse of the wave function to a single determinantal form. The amount of nondynamic electron correlation accounted for by a BS-UDFT description can be directly assessed from the rotational angle θ driving the mixing of HOMO and LUMO. Since for a given problem, it may be difficult to determine the optimized θ value and the exact form of Eq. (4), it is easier to calculate the natural orbitals of the BS-UDFT wave function.[81,99] The fractional values

 © 2013 John Wiley & Sons, Ltd.

TABLE 1 | Energetics of the Bergman Cyclization of **1**

Method/Basis Set	$\Delta E^{\ddagger}(1-2)$		$\Delta E^{\ddagger}(2-1)$		$\Delta_R E$		T-S		Ref.
		Sum[a]		Sum[a]		Sum[a]		Sum[a]	
SVWN/cc-pVTZ	19.2	17.1	18.6	18.6	6.8	8.8	0.6	−1.5	43
BP86/cc-pVTZ	24.6	21.9	18.6	18.6	4.0	6.7	6.0	3.3	43
BPW91/cc-pVTZ	25.4	22.8	20.0	20.0	3.6	6.3	5.4	2.8	43
BLYP/cc-pVTZ	28.6	25.8	15.1	15.1	4.5	7.3	13.6	10.8	43
B3PW91/cc-pVTZ	31.2	29.0	28.5	28.5	2.4	4.6	2.7	0.5	43
B3LYP/6-31G(d,p)	31.2	28.9	27.9	27.9	2.5	4.7	3.3	1.1	43
B3LYP/cc-pVTZ	34.4	32.1	24.3	24.3	2.6	4.9	10.1	7.8	43
B3LYP1/6-31++g(3df,3pd)	34.1	31.8	24.0	24.0	2.6	4.9	10.1	7.8	43
CCSD(T)/6-31G(d,p)	29.5		24.0		5.5		2.5		56, 98
Experimental [b]	30.1 ± 0.5		22.2 ± 0.7		7.8 ± 1.0		3.5 ± 0.5		42, 44

Method/Basis Set	$\Delta H^{\ddagger}(1-2)$	$\Delta H^{\ddagger}(2-1)$	$\Delta_R H$	T-S	Ref.
CCSD(T)/cc-pVDZ	27.1	23.0	4.1		19
CCSD(T)/cc-pVTZ	27.9	19.4	8.5		100
BD(T)/cc-pVTZ	28.9	18.6	10.3	3.4	19
CASSCF/ANO	43.6	15.9	27.7	3.0	101
GVB-PT2/6-31G(d)	34.8	35.5	−0.7		102
CAS(12,12)PT2/ANO	23.9	20.1	3.8		103
CAS(10,10)PT2/ANO-L	25.2	15.7	9.5		104
CAS(12,12)PT2/ANO-L	25.0	16.4	8.6		104
MRCI/cc-pVTZ	29.4	19.1	10.3		100
MRBWCCSD/cc-pVTZ	32.7	19.9	12.9		100
Experimental	28.7 ± 0.5	20.2 ± 0.7	8.5 ± 1.0	3.8 ± 0.5	42, 44

[a] Sum formula according to Eq. (7) used.
[b] Experimental enthalpies corrected to energies at 0 K.

of the natural orbital occupation numbers of the mixing orbitals provide then a simple measure of the amount of nondynamic electron correlation covered by the BS-UDFT wave function.[81] This depends however on the XC functional used.

In Table 1, some selective BS-UDFT results are compared with the experimental values of Roth and co-workers,[42] which have been corrected to energies at 0 K without zero-point energy using calculated vibrational frequencies.[43] The stationary points of the Bergman reaction were first calculated with RDFT, then each RDFT solution was tested with regard to its internal and external stability.[105,106] The singlet state of the biradical turned out to be externally unstable thus indicating a breaking of the constraint $\psi_\alpha = \psi_\beta$. The eigenvector associated with the negative eigenvalue of the stability matrix leads outside the restricted subspace thus yielding a UDFT energy lower than the RDFT energy.

The reliability of the BS-UDFT description of the S state of biradical **2** can be improved by applying the sum rule.[107,108] The sum formula is based on the assumption that (i) the expectation value $\langle \hat{S}^2 \rangle$ can be calculated from KS orbitals and (ii) the predominant contamination of the S state results from a low-lying T state. Then, the BS-UDFT energy of **2S** can be corrected according to Eqs. (6) and (7).

$$E(UDFT, \mathbf{2S}) = x\ E(\mathbf{2S}) + (1-x)\ E(\mathbf{2T}) \quad (6)$$

$$E(\mathbf{2S}) = \frac{1}{x}\ E(BSUDFT, \mathbf{2S}) - \frac{(1-x)}{x}\ E(\mathbf{2T}) \quad (7)$$

where x is determined with Eqs. (8) and (9):

$$\langle \hat{S}^2 \rangle_{BSUDFT,\mathbf{2S}} = x\ \langle \hat{S}^2 \rangle_{\mathbf{2S}} + (1-x)\ \langle \hat{S}^2 \rangle_{\mathbf{2T}} \quad (8)$$

$$x = \frac{\langle \hat{S}^2 \rangle_{BSUDFT,\mathbf{2S}} - \langle \hat{S}^2 \rangle_{\mathbf{2T}}}{\langle \hat{S}^2 \rangle_{\mathbf{2S}} - \langle \hat{S}^2 \rangle_{\mathbf{2T}}} \quad (9)$$

As can be seen from Table 1, the sum formula improves results, especially by reducing the S-T splitting, which comes out too large at the BS-UDFT level. In general, results obtained with a hybrid functional are closer to experiment on the average than those obtained with a GGA functional. This is due to the fact that the SIE error of the latter and the implicit two-configurational character of the BS-UDFT solution lead to a double-counting of correlation

© 2013 John Wiley & Sons, Ltd.

errors.[89] The DFT work on the Bergman cyclization suggests that the performance of BS-UDFT has to be evaluated by referring to the total and on-top pair density distributions rather than the KS orbitals and the spin density distribution because the former do not suffer from the symmetry-breaking problem.[43]

The description of the Schreiner–Pascal biradical **3** (Figure 1), which is essentially a 1,4-butadienyl biradical stabilized by through-bond interactions involving the bonding and antibonding $\sigma(C4C5)$ orbitals, is more challenging than that of *p*-benzyne **2** because of the branching points in the conjugated system and the lower symmetry. Nevertheless, BS-UDFT with an appropriate XC functional can also provide in this case reasonable results.[19]

Permuted Orbital UDFT Description of the Meyers-Saito Biradical

The situation is however different in the case of the $\sigma-\pi$-radicals **5** and **6**. A BS-UDFT description is not useful, which can be explained by considering the σ,π-OSS $^1B_1$ state of methylene as a prototype for such a biradical. In the $^1B_1$ OSS state of methylene, the electron with α- (β-)spin can occupy either the σ (π) or the π (σ) orbital and both possibilities have to be included into the wave function thus leading to a two-determinantal CSF without any nondynamic electron correlation; there is just dynamic electron correlation (type I system in Figure 8). KS-DFT as a single-determinant method cannot describe the two-determinantal wave function. There is however a possibility of handling such a problem in form of a PO-UDFT calculation.[81,99]

When constructing the PO-UDFT wave function, the order of the orbitals is changed for one of the spin orientations, for example, by exchanging HOMO and LUMO for the β spin orientation. This leads for the open-shell part of the OSS state of methylene according to Eq. (10):

$$\Psi_{\text{open}}^{\text{PO-U}} = |\psi_\sigma \overline{\psi_\pi}\rangle \tag{10}$$

The resulting initial state is a mixture of a $\sigma\pi$ singlet and a $\sigma\pi$ triplet component with equal weights:

$$\left|\psi_\sigma \overline{\psi_\pi}\right\rangle = \frac{1}{\sqrt{2}}\left(|\psi_\sigma \overline{\psi_\pi}\rangle^T + |\psi_\sigma \overline{\psi_\pi}\rangle^S\right) \tag{11}$$

$$|\psi_\sigma \overline{\psi_\pi}\rangle^S = \frac{1}{\sqrt{2}}\left(|\psi_\sigma \overline{\psi_\pi}\rangle + |\psi_\pi \overline{\psi_\sigma}\rangle\right) \tag{12}$$

$$|\psi_\sigma \overline{\psi_\pi}\rangle^T = \frac{1}{\sqrt{2}}\left(|\psi_\sigma \overline{\psi_\pi}\rangle - |\psi_\pi \overline{\psi_\sigma}\rangle\right) \tag{13}$$

The correct two-determinantal wave function of the OSS state is contained in the PO-UDFT wave function so that the $^1B_1$ state of methylene can be adequately described. However, the price for recovering the singlet state within the single-determinantal PO-UDFT wave function is a contamination by the two-determinantal triplet component with $M_S = 0$. Superposition of singlet and triplet components breaks the spin symmetry of the closed-shell initial state. With regard to the spatial symmetry, the PO-UDFT reference state will belong to a one-dimensional irreducible representation ($^{1,3}B_1$), which is antisymmetric with respect to the symmetry plane containing the molecule.

The σ,π-biradical **5** and **6** of the Myers–Saito or Schmittel reaction are type III rather than type I systems. This results from a mutual spin-polarization of the two unpaired electrons. Type III systems (Figure 8) require a two-determinantal, two-configurational description, i.e. the wave function can only be represented by two (or more) CSFs Ψ_0, Ψ_1, etc., each of which must be spanned by two (or more) Slater determinants Φ_i, Φ_i', etc. The Meyers biradical (α-3-didehydrotoluene, Figure 8) possesses a singlet ground state because of spin polarization effects between the unpaired electrons. Both normal RDFT, UDFT, BS-UDFT, or PO-UDFT fail in such a situation. Possible are only DFT methods, which explicitly include multireference effects.

Description of Biradicals with ROSS, REKS, and CAS-DFT

ROSS is limited to the application of σ,π-biradicals. The method yields for biradical **5** a reasonable geometry, however fails to predict the singlet to be more stable than the triplet, which indicates that spin-polarization is not correctly described. REKS is limited to a (2,2) active space, which excludes a reasonable account of the energetics of the Bergman or Meyers–Saito reaction. However, Cremer and co-workers used REKS(2,2) to calculate the singlet–triplet splitting of biradical **2**.[81,99] A value of 2.5 kcal/mol (see Table 2) was obtained provided a hybrid functional such as B3LYP was used. The method leads to much larger values with pure XC functionals reminiscent of a double counting of correlation effects in the case of the singlet.[81,99] The most promising results have been obtained with CAS(8,8)DFT (for singlet–triplet splittings) and CAS(12,12)DFT (for the energetics of the Bergman reaction).[86–88] In the latter case, however results clearly suffer somewhat from the shortcomings of the CASSCF approach, which cannot be offset by the DFT correlation functional. It is of course of advantage that CAS-DFT can describe reasonably

 © 2013 John Wiley & Sons, Ltd.

TABLE 2 | Energetics of the Myers–Saito and Schmittel Cyclization of **4**

Method/Basis Set	$\Delta H^{\ddagger}(4-5)$	$\Delta H^{\ddagger}(5-4)$	$\Delta_R H$	T-S	Ref.
UBS-B3LYP/6-31G(d,p) [a]	24.0	37.6	−13.6		19
REKS-BLYP/6-31G(d)	20.0	28.3	−8.3		109
PO-UDFT-B3LYP/6-31G(d)				−1.0	81
CAS(8,8)-DFT/6-31G(d)				−2.5	81
UHF-CCSD(T)/6-31G(d,p)	22.3	34.7	−12.4		110
UHF-BD(T)/6-31G(d,p)	22.3	36.4	−14.1		110
CASSCF(10,10)/6-31G(d,p)[b]	31.1	34.2	−3.1		50
MRMP2/6-31G(d,p)[b]	17.4	32.4	−15.0		50
MRMP2/6-311+G(d,p)[b]	16.9	30.9	−14.0		50
MR-CI+Q/6-31G(d) [c]	27.9	44.0	−17.0		111
Experimental	21.8 ± 0.5	36.8 ± 2.5	− 15 ± 3	-5	112

Method/Basis Set	$\Delta H^{\ddagger}(4-6)$	$\Delta H^{\ddagger}(6-4)$	$\Delta_R H$	T-S	Ref.
UBS-B3LYP/6-31G(d,p) [a]	31.4	42.3	10.9		19
REKS-BLYP/6-31G(d)	33.4	49.9	16.5	3.2	109
CASSCF(10,10)/6-31G(d,p)[b]	39.1	61.2	22.1		50
MRMP2/6-31G(d,p)[b]	42.0	34.9	10.9		50
MRMP2/6-311+G(d,p)[b]	22.9	33.4	10.5		50
MR-CI+Q/6-31G(d) [c]	35.0	47.0	12.0	5.0	111

[a] Free energy differences are given.
[b] Energy differences including ZPE (zero-point energy) corrections are given.
[b] Energy differences are given.

any of the three biradical formation reactions, which is not true for either BS-UDFT, REKS, or ROSS.

Single Reference Coupled Cluster Theory

Correlation-corrected wave function methods usually start from the HF mean-field orbitals. Hence the shortcomings of the HF orbitals have to be gradually corrected at the correlated level by the single (S) excitations and their coupling to other excitations effects. This will be effective if the infinite order effects of CC theory are included, and these are coupled to the important double (D) excitations describing pair correlation effects so that in the space of the S and D excitations a full configuration interaction (FCI) quality is achieved within a CCSD calculation.[113] If a CCSD (CC with all S and D excitations) approach is augmented by perturbative triple (T) excitations (CCSD(T)),[15] there are terms in the CC expansion, which account for the multireference character of type II systems (see Figure 8).[114,115] For example, a disconnected quadruple (Q) term can describe the pair correlation for the doubly excited configuration Φ_1 of *p*-benzyne. Also, the three-electron effects accounted for by the T excitations can describe through-bond delocalization effects of the *p*-benzyne biradical appropriately so that a balance between biradical and closed-shell character can be provided.[115]

There is however a significant difference whether to perform the CC calculation of the *p*-benzyne with a spin-restricted or a spin-unrestricted CC ansatz. For example, spin-restricted CCSD(T) (RCCSD(T)) provides reasonable energies and geometries for the Bergman cyclization of the parent enediyne **1**, as was first demonstrated by Kraka and Cremer.[56,98] However, it fails to describe second-order and higher order response properties of *p*-benzyne such as harmonic vibrational frequencies or infrared intensities.[116] This is a result of orbital instability effects caused by the existence of low-lying excited states, which can mix with the ground state in the sense of a pseudo-Jahn–Teller effect (PJTE).[117] A second-order expression for describing the energy effects of this orbital instability can be obtained by a Taylor expansion of the molecular energy at the equilibrium geometry for a given normal mode coordinate Q_μ as it is done in the case of the PJTE[117]:

$$E_\mu(2) = \frac{1}{2}\left\langle \Phi_0 \left| \frac{\partial^2 H}{\partial Q_\mu^2} \right| \Phi_0 \right\rangle Q_\mu^2 + \sum_k \frac{\left| \left\langle \Phi_0 \left| \frac{\partial H}{\partial Q_\mu} \right| \Phi_k \right\rangle \right|^2}{E_0 - E_k} Q_\mu^2 \qquad (14)$$

© 2013 John Wiley & Sons, Ltd.

where Φ_0 and Φ_k represent the ^1A_g ground state of **2** and a perturbing state k, respectively. The first term in Eq. (14) involves the diagonal contribution to the quadratic force constant in the absence of the state interaction, and the second term the magnitude of these interactions where $\langle\Phi_0|\partial H/\partial Q_\mu|\Phi_k\rangle$ denotes the vibronic coupling element between ground state and excited state k. The second term will be nonzero only if the direct product of the irreducible representations of Q_μ, Φ_0, and Φ_k contain the totally symmetric representation of the molecular point group. If the perturbing state, Φ_k, lies higher in energy than Φ_0, then the second term in Eq. (14) will be negative and, depending on its magnitude, may cause an energy lowering upon distortion of the molecular geometry along the symmetry-breaking normal mode Q_μ. If either states 0 and k are close in energy thus yielding a small denominator in the second term or the nonadiabatic coupling matrix element in the numerator is significant, the PJTE will be substantial and affect the second order response properties of *p*-benzyne.

It has been shown[116] that the excited $^1B_{1u}$, $^1B_{2g}$, or $^1B_{1g}$ states of *p*-benzyne generated by an electron excitation from the HOMO (b_{1u}), HOMO-1 (b_{2g}), or HOMO-2 (b_{1g}) to the LUMO (a_g) cause a PJTE in combination with normal modes of exactly these symmetries. A measure of the importance of the PJTE is provided by the eigenvalues of the molecular orbital Hessian et al.,[118] i.e. the second derivative of the HF energy with respect to orbital rotations, whose inverse implicitly appears in the second term of Eq. (14). Although none of these eigenvalues was found to be negative, their near-zero magnitudes lead to nonsensical vibrational frequencies and infrared intensities for the three modes with b_{1u}, b_{2g}, and b_{1g} symmetry even for the highly correlated RCCSD(T) wave function. In the case of less correlated approaches such as Møller–Plesset perturbation theory[119,120] at lower order, the deficiencies of the restricted Hartree-Fock starting orbitals cause imaginary harmonic vibrational frequencies. In this connection, it has to be noted that deficiencies of a given correlated method in overcoming the multireference or orbital instability errors when describing the biradicals generated in the course of the cyclization of an enediyne or enyne-allene cannot be compensated by the use of larger basis sets.[116]

The orbital instabilities in the case of *p*-benzyne can be avoided by using either spin-restricted Brueckner orbitals and the BD(T) (Brueckner doubles and perturbative triple excitations) method.[121,122] Brueckner orbitals are obtained by rotating the orbitals in such a way that the S excitations of the CCSD expansion are eliminated, which obviously alleviates the deficiencies of the spin-restricted HF mean-field orbitals. This approach has also been used for describing the σ,π-biradicals of the Myers–Saito and Schmittel reaction after mixing the a'-symmetrical HOMO with the a''-symmetrical LUMO and obtaining in this way better suited delocalized MOs for the BD(T) calculation.[19,123]

Alternatively, one can revert to a spin-unrestricted HF (UHF) description to obtain better suited reference orbitals for the CC calculations, which no longer lead to the orbital instability effects of the spin-restricted orbitals.[116] The problem of spin contamination is not pendant because the triplet contaminants are completely annihilated by the infinite-order (or FCI) effects in the S- and D-excitation space of CCSD and any higher CC method. However, it was also shown[116] that correlation-corrected UHF methods that do not include infinite order effects in the SD-space cannot provide reliable results for *p*-benzyne because of the unusually large spin contamination resulting from two rather than just one triplet state.

The first experimental evidence for the generation of a *p*-benzyne resulted from matrix-isolation spectroscopy[45] where the positive identification of the biradical could only be accomplished by calculating its infrared spectrum (then done utilizing BS-UB3LYP). A RCCSD(T) description, despite the many times larger computational effort, would not have been suitable in this case because of the orbital instabilities of the starting HF wave function. However, an UHF-CCSD(T) description of the IR spectrum fully confirmed the original BS-UB3LYP description. Similar considerations as discussed here for *p*-benzyne also apply to other biradicals such as m-benzyne.[46,47,124]

In Table 1, CCSD(T) and BD(T) activation and reaction enthalpies $\Delta H^{\ddagger}(298)$ and $\Delta_R H(298)$, respectively, for the Bergman cyclization are listed. The CCSD(T)/cc-pVTZ enthalpies[100] deviate by less than a kcal/mol from experiment, whereas the BD(T)/cc-pVDZ enthalpies[19] deviate by maximally 2 kcal/mol, which could result from the use of a BS-UBPW91/cc-pVDZ geometry.

Multireference Descriptions

The first complete active space SCF (CASSCF) calculation by Koga and Morokuma used a (10,10) active space (10 electrons in 10 orbitals) with a basis set of moderate size.[125] CASSCF[126] carries out a FCI calculation for the active space and also optimizes the orbitals. Although it should provide the correct multireference character of σ,σ- or σ,π-biradicals or -biradicaloids, it does not guarantee a reliable account of the energetics of an enediyne or enyne-allene cyclization reaction. First of all, the definition of the active space is a nontrivial problem. Koga and

 © 2013 John Wiley & Sons, Ltd.

Morokuma included the six out-of-plane and the four in-plane π-electrons of the reactant.[125] This however leads to an unbalanced active space for the product because in this case through bond delocalization is described for just one half of the molecule. For a balanced description, the other pair of σ-electrons (contributing to the ene-double bond) has to be included thus leading to a (12,12)-active space. Of course, one could also consider whether geminal interactions between σ-bonds must be included, which would lead to a (20,20)-active space, which is beyond what is possible in a CASSCF calculation today.

CASSCF calculations also fail to describe the Bergman (see Table 1) or any other of the related rearrangement reactions correctly because CASSCF (or multiconfigurational SCF, MCSCF) as well as HF lack the important dynamic electron correlation effects. Therefore, they have to be combined with a dynamic electron correlation method such as configuration interaction (CI) or perturbation theory.

Multireference Descriptions of the Bergman and Related Reactions Including Dynamic Electron Correlation

There are only a few multireference investigations with dynamic electron correlation included, which have investigated both the energetics of the Bergman cyclization and the singlet–triplet splitting of the *p*-benzyne. CASPT2(8,8) (CASSCF with second-order perturbation theory for a eight electron, eight orbital active space) and CASPT2 (10,10) calculations suffer from the shortcomings of an unbalanced active space (see above).[101,104]

The minimum requirement for the active space is fulfilled by CASPT2(12,12) calculations.[103,104] At the CASPT2(12,12)/ANO (atomic natural orbital basis set) level of theory, Lindh and co-workers obtained an activation enthalpy $\Delta H^{\ddagger}(298)$ that is too low by 3 kcal/mol whereas the endothermicity of the reaction was correctly described (see Table 1). This suggests that the stability of the enediyne is underestimated. Most likely, this is a result of an insufficient account of dynamic electron correlation needed for the appropriate description of electron delocalization in the enediyne. In the course of the Bergman cyclization, the number of electron pairs is reduced by one, which leads also to a significant change in the dynamic two- and three-electron correlation effects. Whereas the former are accounted for by CASPT2, the latter are not.

Recently, Sakai and Nishitani[50] carried out a multireference second-order perturbation theory (MRMP2) study of the Myers–Saito reaction using an (10,10) active space and CASSCF(10,10) geometries. They found a C_1-symmetrical transition state (activation energy 16.6 kcal/mol) and a C_s-symmetrical transition state (18.1 kcal/mol) where the first related to the Myers–Saito biradical **5** (reaction energy −16.2 kcal/mol) and the second to **5** with the methylene group standing perpendicular the benzene ring, i.e. to the transition state of methylene rotation. Clearly, the second path via the C_s-symmetrical transition state must bifurcate (caused by rotation of the methylene group) to reach the final product **5**. Although two transition states involving different π-orbitals to form the new C1C6 bond can exist, there is need to confirm these results by a better way of determining the transition state geometries (including also dynamic electron correlation effects). Noteworthy is that the authors[50] also determined different transition states for the Schmittel reaction.

In connection with the MRMP2 results for the Myers–Saito reaction, it has to be mentioned that Carpenter did extensive CASPT2 studies for the same reaction, which he summarized in a 2006 review on nonadiabatic thermal reactions of organic molecules.[127] In this review, he points out that the cycloaromatization of enyne-allene **4** in methanol as a solvent leads to 2-phenylethanol and benzyl methyl ether in a ratio of 1:3. The former product can be expected as a result of H-abstraction from the methyl group of the solvent. According to Carpenter, the latter speaks for the formation of a thermally excited zwitterionic state. However, all attempts to describe such a state by CASPT2 calculations[127] led to excitation energies, which made a thermal transition via a sloped conical intersection unlikely. We note in this connection that the second transition state found by Sakai and Nishitani and an in-plane attack of methanol can explain the formation of benzyl methyl ether without invoking a zwitterionic state.

Considerable progress has been made in the field of multireference coupled cluster (MRCC) theory.[128] A multireference Brillouin–Wigner CCSD/cc-pVTZ study of the Bergman reaction was carried out by Pittner and co-workers[100] who obtained an activation and reaction enthalpy at 298 K of 32.7 and 12.9 kcal/mol (see Table 1), respectively, thus revealing the necessity of including T excitations at the CC level of theory. MR CID(+Q)/cc-pVTZ (Davidson correction for the quadruple effects to obtain size consistency) calculations yielded better results (29.4 and 10.3 kcal/mol).[100]

Singlet–triplet splittings for the three benzynes have been calculated using either Mukherjee multireference CCSD (MkCCSD),[129] general-model-space state-universal CCSD (GMS-SU-CCSD),[130] or

 © 2013 John Wiley & Sons, Ltd.

internally contracted (ic) MRCCSD theory.[131] By including complete basis set corrections obtained for CCSD and zero-point vibrational energy corrections obtained for CCSD(T),[129] a reduced MRCCSD(T) result of 2.1 kcal/mol at the CCSD(T) geometry of *p*-benzyne was obtained for the singlet–triplet splitting. The icMRCCSD led to a value of 1.6 kcal/mol, which would increased by the triple excitations thus approaching the experimental value of 3.8 ± 0.3 kcal/mol.[44] Evangelista and co-workers estimated the error made in their calculation to be 1.5 kcal/mol thus yielding 3.9 kcal/mol for the singlet–triplet splitting in *p*-benzyne.[129]

MR-CISD and MR-averaged quadratic coupled cluster (MRAQCC) theory was used to determine the vertical excitation energies of valence and Rydberg states of *p*-benzyne. Excited states of *p*-benzyne have also been calculated with the GMS-SU-CCSD approach and compared with Mk-CCSD as well as EOM-CCSD results.[130]

In summary, multireference CC methods are appealing methods for an accurate description of the Bergman cyclization; however, the calculations published so far have not reached this objective since the use of large basis sets and the calculation of geometries and vibrational frequencies at this theoretical level are not yet routine.

TARGET-SPECIFIC ENEDIYNE ANTITUMOR DRUG CANDIDATES

Enediynes are secondary metabolites, which are mainly produced by soil and marine microorganisms.[28,36,132] The first structures of natural enediynes were reported in the mid-1980s.[4–6,8,18,133,134] They are masterpieces, designed by nature to protect microorganisms against toxic bacteria and viruses. Natural enediynes show potent antibiotic and antitumor activities with a cytotoxicity comparable to or even higher than that of any known microbial metabolite.[32,34,135–137] Up to date, ca. 40 different natural enediynes have been found.[28] Some commonly known enediynes[133,134,138–148] are summarized in Table 3 and Figure 11(a) and (b). All natural enediynes possess an unsaturated core containing two alkyne units conjugated with a double bond. This core is embedded into either a 9- or 10-membered ring, and the whole unit (given in blue and purple in Figure 11(a) and (b) is often called the *enediyne warhead* because it is responsible for the biological activity of the natural enediyne. The warhead is connected to a docking unit, which helps the compound to dock into the minor groove of DNA. Furthermore, there is a triggering device, which, if appropriately stimulated by environmental factors, triggers the warhead to undergo a Bergman cyclization. Warhead, triggering device, and docking unit are indicated in Figure 11(b) for calicheamicin.

9-membered ring enediynes (see, e.g., molecules **23–29** in Table 3 and Figure 11(a)) are highly strained, and therefore are only stable if they are bound to an apoprotein.[63] While enediynes incorporated in a 10-membered ring are stable enough to be isolated,[137] the 9-membered ring enediynes without apoprotein undergo spontaneous cycloaromatization leading to the exclusive isolation of aromatized derivatives.[63] This applies to neocarzinostatin (**23**), C-1027 (**24**), maduropeptin (**25**), kedarcidin (**26**), and the precursors of sporolides (**28**) and cynaosporasides (**29**). The only known stable 9-membered ring enediyne without apoprotein is N1999A2 (**27**).[165] The enediynes included in a 10-membered ring (see, e.g., molecules **30–35** in Table 3 and Figure 11(b)) can be divided into (i) enediynes containing a sugar moiety (esperamicin (**30**), calicheamicin (**31**), namenamicin (**33**), shishijimicin (**34**)) and (ii) enediynes containing an antraquinone moiety (dynemicin (**32**), unialamycin (**25**)). The total synthesis of the naturally occurring enediynes was actively pursued in the 1980s and 1990s by organic chemists inspired by the unusual and diverse structures of these compounds. For more detailed discussions, the reader may refer to recent review articles[29,61,62,166] and the original literature cited in Table 3.

Apart from the many challenges caused by the total synthesis of naturally occurring enediynes, there is also the challenge of understanding how nature created their structure, i.e. how one can reconstruct their biosynthesis.[32,167] Townsend and co-workers investigated the function of the polyketide synthases responsible for the "programmed" synthesis and regioselective cyclization of linear precursors.[168–170] This led to new insights into how the polyketide synthases are involved in the biosynthesis of calicheamicin. In addition, their research shed light into the divergence to 9- or 10-membered natural enediynes, which results, according to the authors, from the action of one or more accessory enzymes acting in concert with the enediyne polyketide synthases.

The gene clusters for **23**, **24**, **25**, **31**, and **32** have been cloned and sequenced[167] thus providing the basis for understanding nature's means to create such complex, exotic molecules. Sequencing of the gene clusters could confirm the polyketide origin of the enediyne warheads. Aromatic moieties are derived either from polyketides or primary metabolic intermediates, whereas the unusual sugars are a result

 © 2013 John Wiley & Sons, Ltd.

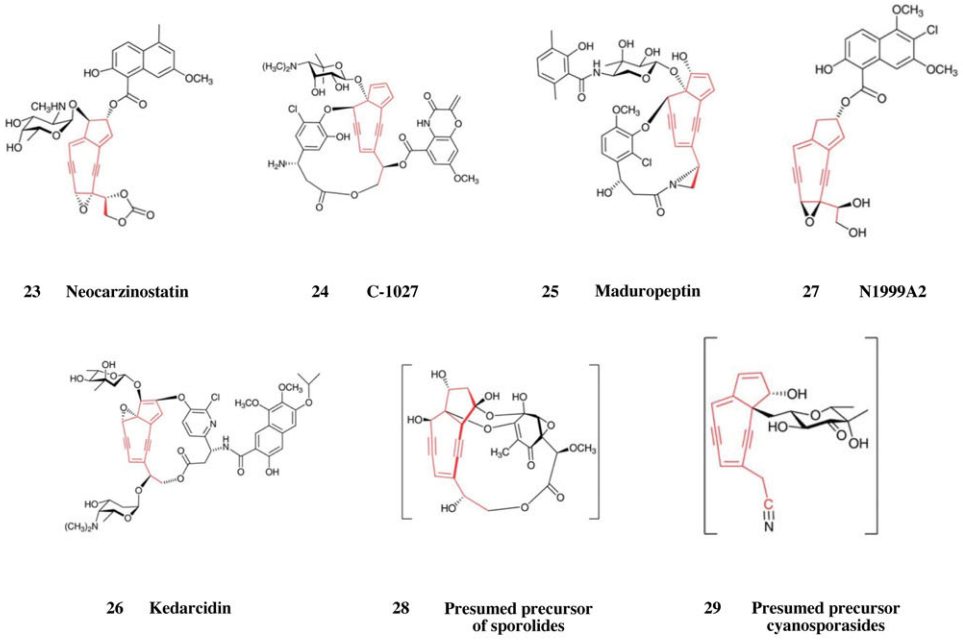

(a) Nine-memberedenediynes.

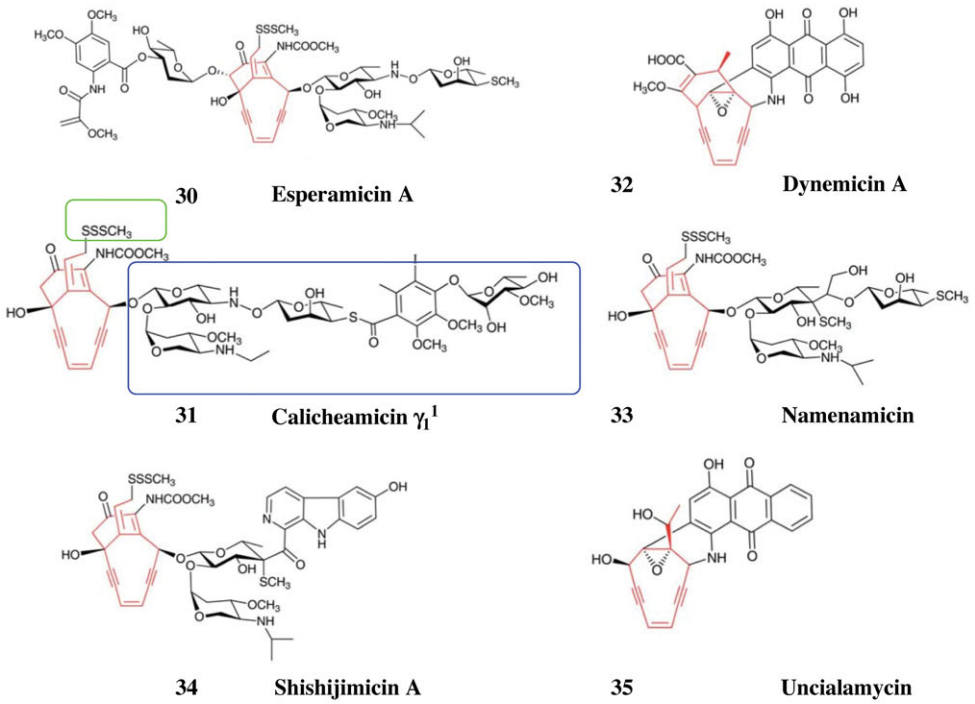

(b) 10-Membered enediynes.

FIGURE 11 | Naturally occurring enediynes. For each enediyne, the warhead is given in red. For calicheamicin γ_1^1, the docking (blue box) and the triggering device (green box) are also indicated.

© 2013 John Wiley & Sons, Ltd.

TABLE 3 | Some Representative Natural Enediynes.

Compound	Biological Origin	First Structure	Total Synthesis
9-membered ring			
Neocarzinostatin **(23)**	*Streptomycescarzinostaticus* (terrestrial)	1985[133]	1985[149]
C-1027 **(24)**	*Streptomycesglobisporus* (terrestrial)	1991[138]	1985[150]
Maduropeptin **(25)**	*Actinomaduramadurea* (terrestrial)	1994[139]	1985[151]
Kedarcidin **(26)**	*ActinomyceteL585 – 6* (terrestrial)	1997[140]	1985[152]
N1999A2 **(27)**	*Streptomycessp.AJ9493* (terrestrial)	1998[141]	1985[153]
Sporolides[b] **(28)**	*Salinisporatropica* (marine)	1985[142]	1985[154]
Cyanosporasides[b] **(29)**	*Salinisporapacifica* (marine)	1985[143]	1985[155]
10-membered ring			
Esperamicin **(30)**	*Actinomaduraverrucosospora* (terrestrial)	1985[134]	1985[156]
Calicheamicin **(31)**	*Micromonospora echinospora ssp. calichensis* (terrestrial)	1985[144]	1985[157–159]
Dynemycin **(32)**	*Micromonosporachersina* (terrestrial)	1985[145]	1985[160,161]
Namenamicin **(33)**	*Polysyncratonlithostrotum* (marine)	1985[145]	1985[162]
Shishijimicin **(34)**	*Didemnumproliferum* (marine)	1985[147]	1985[163]
Uncialamycin **(35)**	*Unknown* (marine)	1985[148]	1985[164]

of a modification of common sugars carried out by special enzymes. It seems that all building blocks are assembled separately and joined together in the final stage with the help of regioselective enzymes; however, details are not understood yet. There are also open questions concerning the determinants leading to a 9- versus 10-membered ring in the biosynthesis of the enediyne warhead.

Although structurally diverse, all naturally occurring enediynes share the same, unique mode of action leading to apoptosis caused by DNA cleavage. Enediynes intercalate into chromosomal DNA in a sequence-specific fashion.[34,132,136] The specific chemistry of triggering and docking device of an enediyne fine-tunes its biological activity, which is driven by the enediyne warhead and which determines its cytotoxicity. Triggered by an environmental change such as thiol activation or ultraviolet light, the enediyne core undergoes a Bergman cyclization to yield a benzenoid biradical. The biradical abstracts hydrogen atoms from DNA generating in this way a carbon-centered radical in the ribose part. In the presence of O_2, the DNA will undergo facile double- or single-stranded cleavage through an oxidative radical mechanism causing cell death.[18,171]

The research on enediynes had a strong impact on the development of antitumor drugs in so far as it followed a rational design strategy based on nature rather a trial and error approach.[32,34,135–137] At an early stage, it became clear that the bioactivity of the enediynes could be used to destroy tumor cells and this expectation inspired and challenged the synthesis of bioactive enediynes.[33,61,166,172]

Much of the early work on natural enediynes overlooked the fact that they are highly toxic because they do not discriminate between normal and tumor cells, i.e. natural enediynes are not target specific. There are two basic approaches for solving the toxicity problem: (i) the design of artificial target-specific enediyne mimics and (ii) the modification of natural enediynes to make them target specific. If the modifications are constrained to the warhead, the natural docking and triggering device will not be affected and can be used. In any case, one has to develop a strategy how the enediyne shall differentiate between normal and cancer cells.[173–177]

The Design of Artificial Target-Specific Enediyne Mimics

Different strategic routes have been pursued for the rational design path of pH-triggered enediynes, where attempts have been inspired by the triggering mechanisms applied by nature (for a recent summary, see Basak and co-workers[33]). Common to the four strategic routes A, B, C, and D (see Figure 12) discussed in the following is the idea that a nonreactive precursor is converted by a pH change (acidic or basic medium) into an enediyne or enyne-allene. In the case of a change toward a more acidic medium, the bioactivity of the enediyne mimic is in line with the fact that cancer cells are slightly acidic.[178] However, there is only a gradual lowering of the pH in the cancer cell compared to that in the normal cell (see below). In so far those strategies, which are based on a lowering of the pH, have to be scrutinized whether the lowering required is beyond that what is possible

 © 2013 John Wiley & Sons, Ltd.

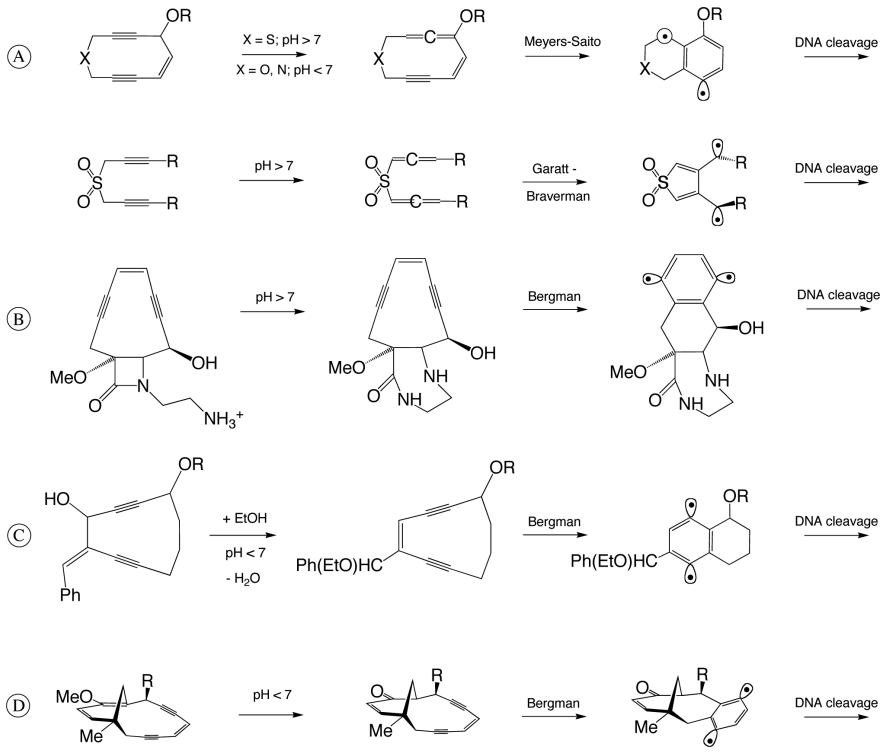

FIGURE 12 | Suggested strategies for biradical formation of an enediyne mimic or related compounds via a precursor at ambient conditions to yield DNA cleavage.

in the cancer cell. As for the alternative strategy (increasing the pH), a direct use as a potential antitumor drug is difficult to foresee. This has to be kept in mind when evaluating the many enediyne mimics synthesized.

Route A: Enyne-Allene Principle

This strategic route makes use of the fact that the barrier of the Myers–Saito cyclization (21.8 kcal/mol, Table 2) is lower than that of the Bergman cyclization (28.7 kcal/mol, Table 1). When triggered by a change in pH, a stable precursor isomerizes to an enyne-allene (see A in Figure 12), which performs a Myers–Saito rearrangement under physiological conditions. Two examples are given in Figure 12. A sulfide with two propargyl groups embedded in a 10-membered ring rearranges under basic condition. The corresponding aza and oxo analogues carry out the cylization under acidic conditions.[179] Shibuya and co-workers[180] designed enediyne model compounds, which isomerize to enyne-allenes and generate toluene biradicals under acidic conditions. Tuesuwan and Kerwin[172] synthesized 4-aza-3-ene-1,6-diyne systems with pH-dependent DNA-cleavage activity.

Interesting in this connection is the Garatt–Braverman cyclization, which involves a double allene reaction with subsequent biradical formation.[181] As an example, the rearrangement of a bispropagyl sulfone is shown in Figure 12, which isomerizes in alkaline media to an allenic sulfone and then transforms into a bioactive biradial at ambient temperatures.[181]

Route B: Locking Principle

The strategy of this route is to stabilize the enediyne by fusion to a locking device (e.g., the four-membered ring shown in B, Figure 12) such as an epoxide as in dynemicin[145] (Figure 11(b)). If equipped with a pH-sensitive trigger, the locking device opens in an acidic medium and sets a reactive enediyne free. The example shown in Figure 12 includes a substituted β-lactam, which forms an ammonium ion in acidic medium, but requires then a basic medium to open the lactam ring by in an intramolecular, nucleophilic substitution to a six-membered ring, which activates the Bergman reaction in the annelated 10-membered ring.[33,182]

Route C: Activation of Prodrug Principle

The strategic principle of this route is based on the *in situ* generation of the enediyne through an allylic

 © 2013 John Wiley & Sons, Ltd.

rearrangement, which is triggered in acidic medium. The serendipitous finding that maduropeptin chromophore (**25**), when being extracted with methanol, transforms into a reactive enediyne via an intramolecular nucleophilic attack of the alcohol[139] has motivated this synthetic route. It has been applied, for example, by Dai and co-workers[183] as shown in Figure 12. A related strategy is the *in situ* generation of an enediyne via β-elimination.[184]

Route D: Rehybridization Principle

Calicheamicin[134] and esperamicin[144] are triggered by a conversion of an sp^2-hybridized carbon into a sp^3-hybridized carbon. The rehybridization strategy has been utilized for pH triggering. For example, Semmelhack and co-workers[185] designed enol-enediynes with a CC double bond at a bridgehead position (see route D in Figure 12). Conversion of the enol into the corresponding keto form under acidic conditions leads to the desired rehybridization. The resulting ketone undergoes Bergman cyclization at physiological conditions.

Modification of Natural Enediynes

The modification of the warhead of the naturally occurring enediynes has been sparsely pursued so far. This more "top-down" approach implies the detailed understanding of the mechanism leading to biologically activity of a natural enediyne. In addition, one has to investigate all changes in the biological activity of the enediyne upon altering the warhead. This is a tedious task with an uncertain outcome when based on chemical synthesis. Therefore, computational chemistry plays an important role since it can be used for a better understanding of the mechanism leading to the bioactivity of natural enediynes as well as the monitoring of changes in this mechanism upon modification of the warhead. In view of the size of the natural enediynes, molecular mechanics (MM) investigations have focused on their conformational flexibility.[137,177] MM calculations however can say little with regard to the biological activity of a natural enediyne because this involves bond formation/cleavage, which can only be described utilizing quantum chemical means. There are a few quantum mechanical (QM) and QM/MM (quantum mechanics combined with molecular mechanics) studies of natural enediynes, which will be considered first before the work on a possible modification of their warheads is reviewed.

Computational Investigation of Natural Enediynes

Extensive work on dynemicin and calicheamicin and their reactions has been published by Kraka, Cremer and co-workers who studied the docking, triggering, cyclization, and H-abstraction mechanism inside and outside DNA by appropriate QM and QM/MM methodologies, where the QM part was based on BS-UDFT calculations with the B3LYP hybrid functional.[59,173–175]

Dynemicin A, when locked in its untriggered form via the epoxide unit is predicted to undergo the Bergman cyclization with the extremely high barrier of 52 kcal/mol.[59] When the epoxide ring opens after appropriate triggering, the energy barrier is reduced to 17.9 kcal/mol with the consequence that H-abstraction at ambient temperature becomes possible. If triggering and biological activity of dynemicin A are investigated both inside and outside the minor groove of a duplex 10-mer B-DNA sequence d(CTACTACTGG)·d(CCAGTAGTAG), the importance of a fine-tuning of docking and triggering becomes obvious. Triggering happens in the minor groove in an insertion rather than intercalation mode by NAPDH (nicotinamide adenine dinucleotide phosphate), thiols, or other reducing agents, which are able of attacking a protruding part of the molecule. Triggering is a highly exothermic process that, despite of energy dissipation, should provide a sufficient excess of energy for dynemicin to carry out the Bergman reaction.[173] An important finding of the quantum chemical investigation was that the activity-relevant docking mode is an edge-on insertion into the minor groove, whereas the intercalation between two base pairs, although leading to larger binding energies, excludes a triggering of dynemicin A and the development of its biological activity, as shown in Figure 13.[173]

An insertion–intercalation model was developed that can explain known experimental observations made for dynemicin, especially the observation of the high ratio of single-strand to double-strand scission.[173] In a follow-up study on dynemicin,[175] a state-of-the-art QM/MM calculation revealed that for the Bergman and retro-Bergman cyclization steps of dynemicin the explicit consideration of environmental factors such as the receptor DNA, the solvent water, and charge neutralization by counterions has only minor effects on the energetics of the cyclization, which is obviously due to the cyclic structure of the enediyne investigated. In this case, the energetics is predominantly determined by QM (electronic) effects. This makes a cost-effective

 © 2013 John Wiley & Sons, Ltd.

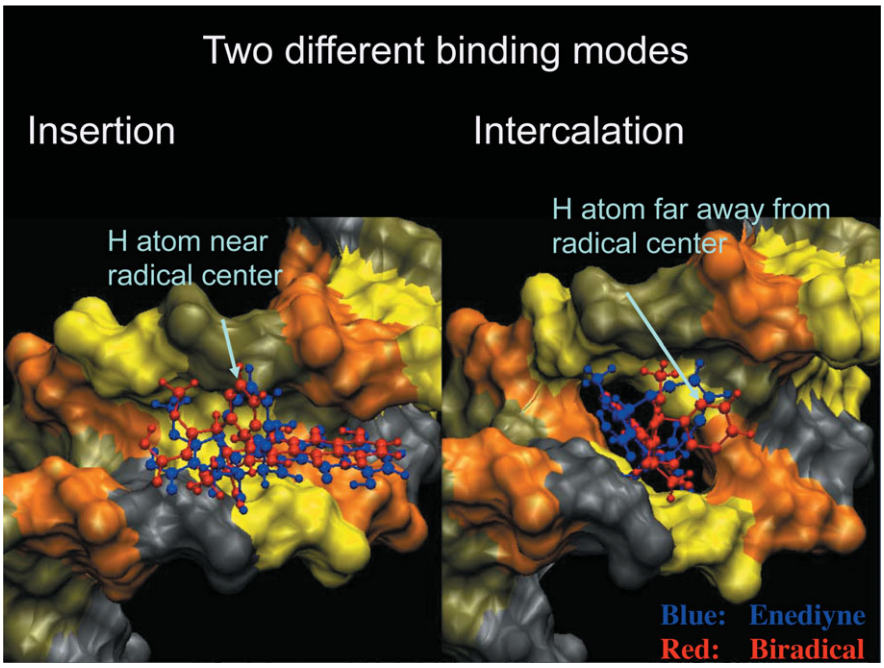

FIGURE 13 | Docking of dynemicin into the minor groove of DNA. (a) Insertion and (b) intercalation. (Reproduced from Ref 173. Copyright 2005, American Chemical Society.)

decoupled QM+MM approach useful for the investigation of natural enediynes.[173,174] For the retro-Bergman cyclization, which involves the acyclic isomer of dynemicin, a lowering of the barrier from 31.3 kcal/mol (gas phase) to 23.7 kcal/mol (inside the minor groove) was found. The lowering of the barrier is reflected by a decrease of the critical distance between atoms C1 and C6 from 4.29 to 3.42 Å.[175] The reduction of the barrier is a result of a stabilization of the transition state, which is caused by an increased dipole moment and hence stronger electrostatic interactions with the environment. This finding proofs the possibility of using acyclic enediynes for drug design if properly anchored in the minor groove.

The triggering and the Bergman cyclization of calicheamicin **31** outside and inside the minor groove of the duplex 9mer-B-DNA sequence d(CACTCCTGG)·d(CCAGGAGTG) was also investigated applying the QM/MM methodology.[174] In contrast to dynemicin, the environment plays a decisive role for the biological activity of calicheamicin, which became clear with the help of QM/MM investigations. Only when calicheamicin is confined to the space of the minor groove triggering leads to a conformation, which performs the Bergman cyclization at ambient temperature whereas outside the DNA calicheamicin is stable. The quantum chemical calculations confirmed the high toxicity of **31**, which performs a DNA double strand scission. There have been investigations on esperamicin; however, in these cases only parts of the molecule were quantum chemically calculated.[186]

Modification of the Warhead of Natural Enediynes: The Role of Heteroenediynes

Any modification of the warhead must have the objective to make the enediyne target specific, i.e. it should attack the tumor rather than the normal cell. This implies that the enediyne must be sensitive to the differences between normal and tumor cell, of which there exist only a few:[178]

i. There is a reduced blood flow in the cancer cell compared to the normal cell. ii. Also the oxygen content is strongly reduced in the cancer cell. iii. Because of the increased nutrition (energy) demand of a tumor cell, glycolysis is strongly enlarged. iv. Owing to the increase in glycolysis, the pH of a cancer cell is lowered to 6.2–6.6 compared to that of the normal cell (pH: 7.0-7.2).[187,188]

There is little chance of exploiting (i)–(iii). However, the lowering of the pH in the tumor cell speaks for the incorporation of a pH sensor into the enediyne warhead. Along these lines, Kraka and Cremer developed an antitumor-enediyne drug principle.[189–191] Clearly, a change in the pH by maximally one unit requires an extremely sensitive chemical pH-measuring device although MCT (monocarboxylate transporters) inhibitors, hyperthermia, or hyperglycemia may lower the pH of the tumor cell to even 5.5 (even lower pH values lead to cell

 © 2013 John Wiley & Sons, Ltd.

TABLE 4 | Energetics of the Bergman Cyclization of (*Z*)-aza-hex-3-ene-1,5-diyne (**37**) to the Corresponding Biradical **38** and the Protonated Form of **37** (**39**) to the Corresponding Protonated Biradical **40**

Method/Basis Set	$\Delta H^{\ddagger}(37-38)$	$\Delta H^{\ddagger}(38-37)$	$\Delta_R H$	T-S	Ref.
BS-UPW91/cc-pVDZ	14.5	29.0	−14.5	14.0	195
BS-UB3LYP/6-31+G(3df,3pd)	23.8	35.9	−12.1	9.1	56
CCSD(T)/cc-pVDZ	17.5	28.2	−10.7	12.9	195
BD(T)/cc-pVDZ	17.4	27.2	−9.7	11.6	195
CASSCF(6,6)/6-31G(d)[a]	33.2	32.7	0.5	6.3	102
CASPT2(10,10)/cc-pVDZ	16.3	36.1	−19.8	14.1	195
CASPT2(12,11)/ANO-S	15.1	27.6	−12.5		104
CASMP2(6,6)/6-31G(d)[a]	27.7	39.8	−12.1	8.2	102
Experimental	22.5 ± 0.5		na	na	102

Method/basis set	$\Delta H^{\ddagger}(39-40)$	$\Delta H^{\ddagger}(40-39)$	$\Delta_R H$	T-S	Ref.
BS-UPW91/cc-pVDZ	18.3	25.2	−6.9	4.3	195
BS-UB3LYP/6-31+G(3df,3pd)	27.9	27.0	−0.9	3.8	56
CCSD(T)/cc-pVDZ	19.9	50.5	−30.6	29.8	195
BD(T)/cc-pVDZ	19.9	25.8	−7.0	5.6	195
CASSCF(6,6)/6-31G(d)[a]	32.5	30.4	2.1	2.2	102
CASPT2(10,10/cc-pVDZ	18.2	33.3	−15.1	5.6	195
CASMP2(6,6)/6-31G(d)[a]	29.1	40.9	−11.8	2.7	102

[a] ΔE values at 0 K.

death[192–194]). It was obvious that a pH sensitive group must be a heteroatom such as nitrogen, which, when incorporated into the enediyne framework and protonated, leads to a varying energetics for the Bergman cyclization. Different heteroenediyne systems including N-containing enediynes, related *N*,*C*-dialkynyl amides, and amidines were computationally tested for their suitability as pH sensors. As an example, the energetics of (*Z*)-3-aza-hex-3-ene-1,5-diyne (**37**) is summarized in Table 4, for which, beside the experimental investigation[102] of the activation enthalpy, a larger number of quantum chemical data were published.

As in the case of the parent enediyne **1**, BS-UDFT, if carried out with a large basis set (diffuse functions for the heteroatom), and avoiding a double counting of correlation effects by using a hybrid functional for the broken symmetry approach (see section *Broken Symmetry UDFT Description of* p-*Benzyne*) leads to reasonable results. The CCSD(T) and BD(T) calculations of Cramer[195] suffer from the use of DFT geometries, whereas both CASSCF and CASPT2 are unreliable, which is a consequence of the enhanced difficulties in defining a balanced active space. As was pointed out by Kraka and Cremer[191], there is, beside through-bond interaction, also a(n) (anomeric) three-electron delocalization involving the N electron lone pair and the adjacent C atom with the unpaired electron. Hence, a (14,13) or even (22,21) active space is needed for the CASPT2 description of **37**.

The BS-UDFT results suggest, in line with the experimental observations, that incorporation of an N atom into the enediyne framework as in **37** leads to a lowering of the barrier and an increase of the exothermicity of the reaction ($\Delta H^{\ddagger}$: 23.8 kcal/mol; $\Delta_R H$: −12.1 kcal/mol). The use of **37** in the warhead of a natural enediyne to make it pH sensitive could imply the following advantages: (i) The singlet–triplet splitting (S-T in Table 4) is 9.1 kcal/mol and by this indicative of a biradical with low reactivity, which is a desirable effect because **37** should not react in the neutral medium of a normal cell. (ii) Also favorable is that protonated biradical **40** does not convert back to **37** at room temperature (activation enthalpy for the retro-Bergman reaction: 27.0 kcal/mol, Table 4). It would abstract an H atom from DNA, which requires 6–12 kcal/mol.[176,196] (iii) The protonated biradical **40** should be strongly reactive in view of a S-T splitting of 3.8 kcal/mol.

Although (i)–(iii) are in favor of a warhead based on **37**, the fact that the protonated form **39** has a cyclization barrier of 27.9 kcal/mol, which makes it nonreactive at body temperature, excludes the system **37**,**39** to be used as pH sensor when distinguishing between normal and tumor cells.

Nevertheless, the search for suitable aza-enediynes has been continued. Kerwin and co-workers[197] synthesized a series of 1,2-dialkynylimidazoles. They invested the Bergman

 © 2013 John Wiley & Sons, Ltd.

cyclization of these compounds by experimental and computational means using DFT. Although the Bergman cyclization of these compounds proceeds at ambient temperature, they could not find a correlation between the rate of the Bergman cyclization and the cytotoxicity to A459 cells.[197] They concluded that there is no evidence that the cytotoxicity of these 1,2-dialkynyl-imidazoles is due to DNA cleavage via a biradical. This is in line with a large S-T gap of 9–10 kcal/mol, which was calculated. In contrast to these results, Kerwin and co-workers did find DNA cleavage via the Myers—Saito cyclization for 4-aza-3-ene-1,6-diyne systems.[172]

In view of their investigation of natural enediynes and their experience with heteroenediynes, Kraka and Cremer formulated the following *seven criteria for the design of a pH-dependent, nontoxic natural enediyne*:[189]

i. The original, neutral enediyne must be protonated at a pH between 5.5 and 6.6.
ii. The protonated enediyne must be kinetically stable against decomposition or rearrangement reactions other than the Bergman cyclization.
iii. The protonated enediyne must undergo Bergman cyclization at ambient temperature.
iv. The protonated biracial must be kinetically stable, and H abstraction must be its preferred reaction.
v. The biological activity of the protonated biracial must be high.
vi. The enediyne in question must be easy to synthesize.
vii. The enediyne-based drug must possess the appropriate ADME (absorption, distribution, metabolism, excretion) properties to guarantee an optimal performance as antitumor antibiotics.[198]

The last two criteria are difficult to assess from a chemical point of view because they imply extensive studies in pharmacology. At least with regard to (v) a rule of thumb was established on the basis of quantum chemical studies:[102,189,191] *The biological activity of a biradical is high (low) if its singlet–triplet splitting is low(high)*. This rule follows the observation that, e.g., through-bond delocalization in *p*-benzyne reduces its biradical character, stabilizes the singlet state, and accordingly increases the singlet–triplet splitting. A strongly stabilized singlet biradical is no longer reactive, and therefore the singlet–triplet splitting can be used as a simple indicator for the biological activity of a biradical formed by cyclization of enediyne or enyne-allene.

Another rule, also used by Kraka and Cremer, concerned the bioactivity of the enediyne at ambient temperature, which implies that the Bergman cyclization or any other biradical-producing cyclization takes place at body temperature. These authors used simple considerations based on activation free energies, rate constants, and frequency factor (activation entropy) to estimate that for a significant rate at room temperature, the activation enthalpy should not be higher than 22 kcal/mol.[189]

Based on this experience, Kraka and Cremer designed what they called the *door-handle principle*, which is based on the idea of a nonreactive precursor with a single bond separating the alkynyl groups. Upon protonation, the enediyne unit is established and the system undergoes a Bergman cyclization (see Figure 14). Such a system could be an amide (X = O, Y = NH) or amidine (X = NR, Y = NR). Investigation of 15 molecular systems with the atom combination for X and Y shown in Figure 14[189] revealed that amidines are best suited for this purpose because their pK_a values make it possible that they are protonated at a pH of 5.5–6.5 and their energetics for the Bergman cyclization can be modulated by incorporation into the 10-membered ring system **53** in such a way that they fulfill requirements (i) to (v) set up by Kraka and Cremer.[189]

The first prototype of a pH-dependent natural enediyne by replacing the enediyne moiety in dynemicin by an dialkynyl amidine warhead was suggested on the basis of QM+MM calculations.[176] The resulting dynemicin-amidine (DAD) is biologically not active because is forms an extremely labile singlet biradical that can no longer abstract H atoms from DNA because it rearranges immediately to a cumulene (see Figure 15). However, if protonated, it fulfills all requirements for a pH-sensitive modified natural enediyne, as is reflected by a lowering of the activation enthalpy for the Bergman cyclization from 16.7 (dynemicin A) to 11.5 kcal/mol (protonated DAD), kinetic stability of the singlet biradical formed in the cyclization reaction (retro-Bergman barriers of 20.6 and 14.9 kcal/mol), and an increased H abstraction ability of the singlet biradical in view of a S-T splitting of just 1.4 kcal/mol. In addition, DADs in general show improved docking properties in the minor groove of the duplex 10-mer B-DNA sequence d(CTACTACTGG)·d(CCAGTAGTAG) throughout the triggering and Bergman cyclization process. Unpublished work reveals that with an

 © 2013 John Wiley & Sons, Ltd.

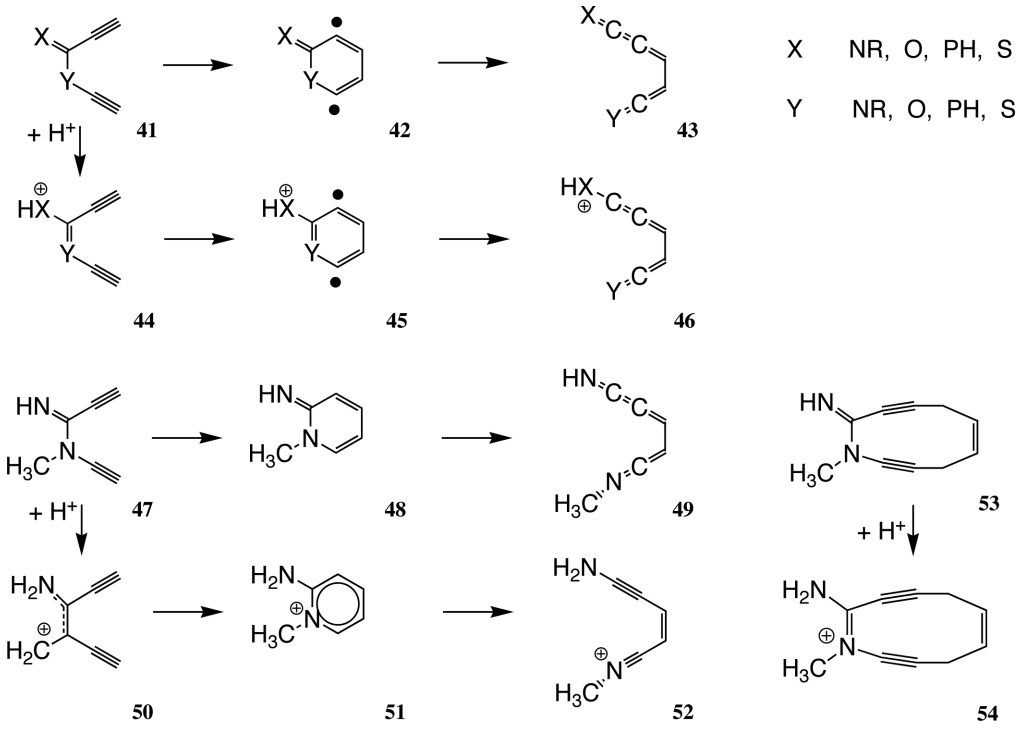

FIGURE 14 | The door handle principle of Kraka and Cremer illustrated for amidines and protonated amidines. (Reproduced from Ref 189. Copyright 2000, American Chemical Society.)

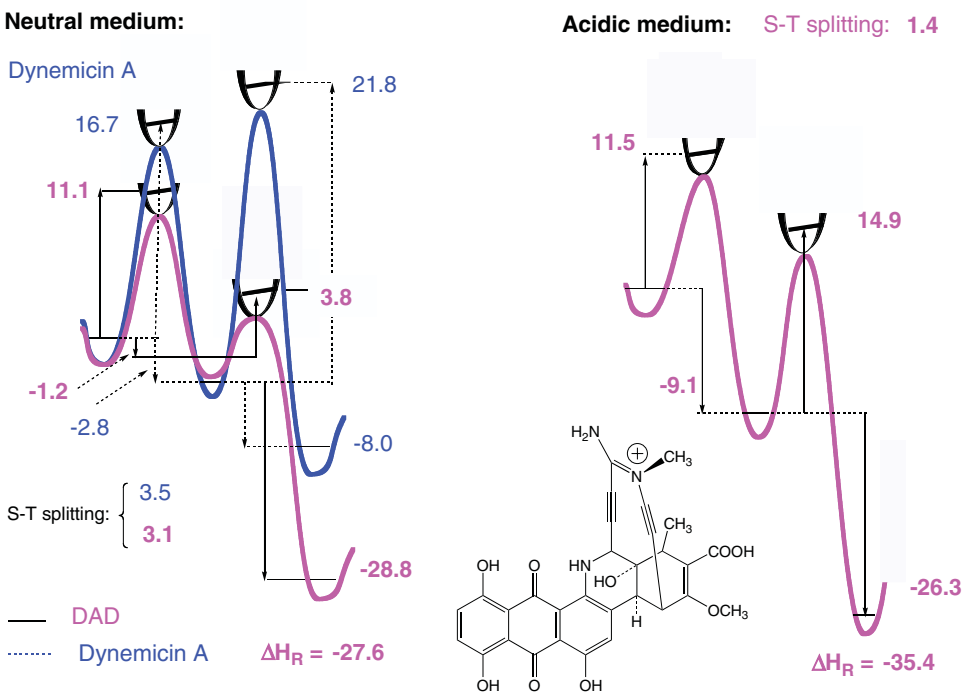

FIGURE 15 | Energetics of dynemicin (blue) versus dynemicin-amidine (DAD; purple). (Reproduced from Ref 176. Copyright 2008, American Chemical Society.)

© 2013 John Wiley & Sons, Ltd.

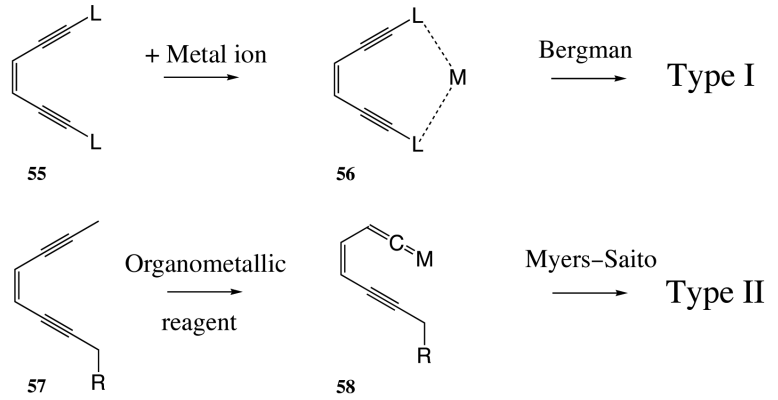

(a) Type I and II reactions

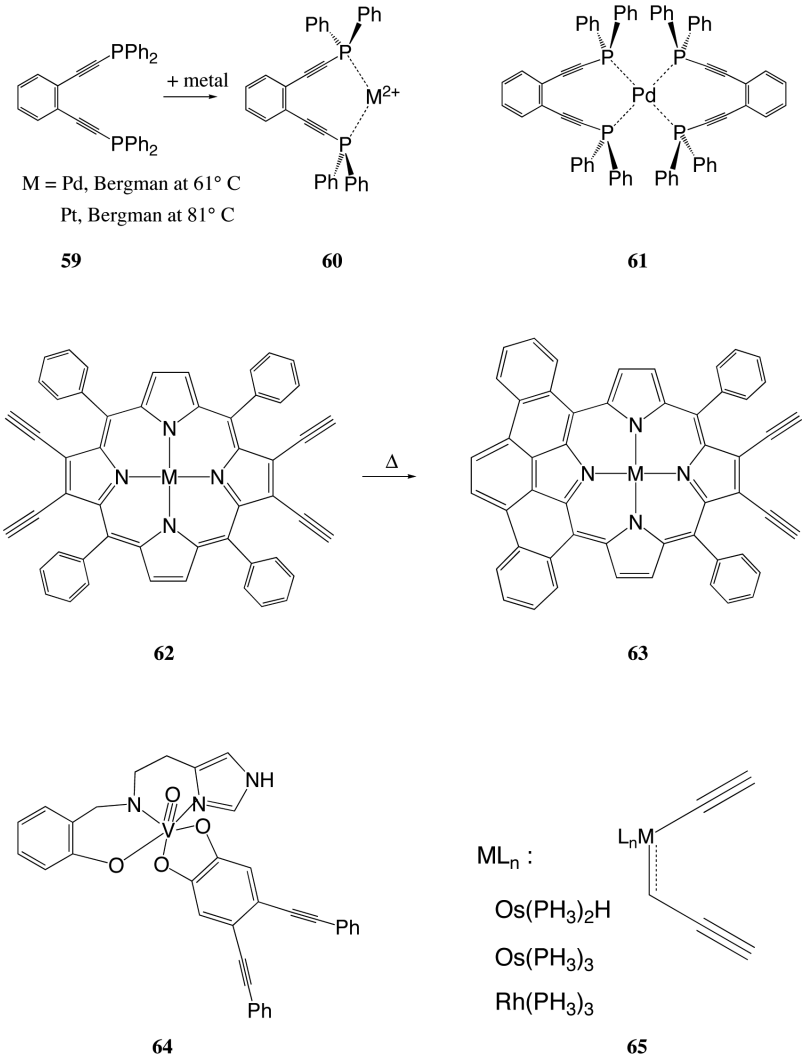

(b) Examples of metalloenediynes

FIGURE 16 | Metalloenediynes investigated to modulate the energetics of the Bergman reaction.

© 2013 John Wiley & Sons, Ltd.

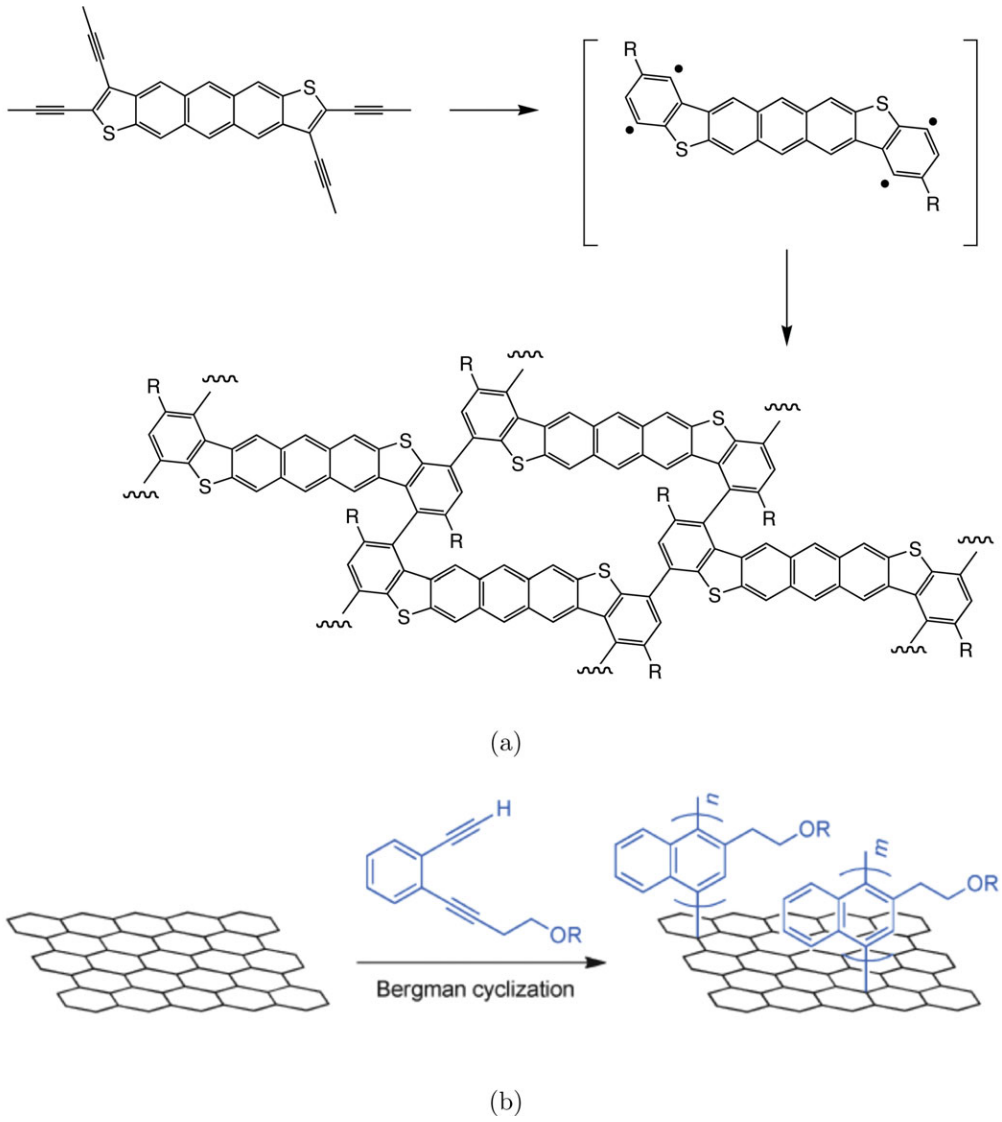

FIGURE 17 | Polymerization of enediynes.

appropriate choice of the amidine substituents the pK_a of a DAD can be fine-tuned to a point that the molecule is protonated in the desired pH range of 5.5–6.5. In this way, an effective anticancer drug based on a nontoxic, pH-sensitive modified natural enediyne can be realized. This work showed also that modification of the warhead is limited. In the case of dynemicin, it does not change the docking properties whereas for calicheamicin it does because of the space requirements of the amidine and the different, tighter docking mode of calicheamicin.[174]

METALLO-ENEDIYNES

The use of metals for a modulation of the Bergman cyclization has become an emerging research field.[28,30,33,51,199] In general, metal sites offer additional structural flexibilities over their carbocyclic or acyclic organic analogues, which contributes to their intriguing Bergman cyclization reactivity. As shown in Figure 16(a), there are two basic modes of action.

Type I; Enediynes **55** bind via their ligands L to a metal ion M^{n+} thus forming a metal-chelated ring **56**, which undergoes the Bergman cyclization.

Type II; Organometallic reagents promote the isomerization of enediyne **57** to enyne-allene **58**, followed by a Myers–Saito cyclization.

In both cases, significant variations in the Bergman cyclization or Meyers–Saito reaction result provided the right choice of the metal is made. Some representative examples will be discussed in the following.

© 2013 John Wiley & Sons, Ltd.

1,2-Bis(diphenyl-phosphino)ethynyl)benzene **59** undergoes the Bergman cyclization at 243°C, as measured by differential scanning caliometry.[200] Complexation with Pd(II) or Pt(II) (see **60** in Figure 16(b)) lowers the barrier considerably so that cyclization takes place at 61° and 81°, respectively. In contrast, the thermal activity of **61** is strongly reduced although both complexes share the same ligand. The main difference is the oxidation state of Pd, which is II in **60** and 0 in **61**. Based on these findings, Zaleski and co-workers[199] have recently designed redox-activated metalloenediyne prodrugs leading to a new strategy for potential dual-thread metalloenediyne therapeutics.

A promising application of metallo-enediynes also exists in the field of photodynamic therapy. Zaleski and co-workers[201] synthesized the vanadium (V) complex **64** (Figure 16(b) with strong ligand-metal charge transfer transitions in the near infrared region caused by the low redox potentials of the highly valent vanadium center and easily oxidizable metal bonds. The Bergman cyclization is activated photochemically using laser light of the wavelength 785 and 1064 nm, respectively, which correspond to wavelengths that ensure enhanced tissue penetration. Recently, the spin-state control of thermal and photochemical Bergman reaction was reported for Pt(II)-dialkynylporphyrin **62**.[202] The thermal Bergman cyclization reactivity of **62** reveals a surprising reduction in the temperature at which the piceno-porphyrin product is formed when compared to Zn(II) derivatives or the metal-free **62**.[203] Hoffman and co-workers[204] investigated the Bergman cyclization of osmaenediynes and rhodaenediynes **65** (Figure 16(b)). Their computational results suggest a potentially significant decrease in the energy of activation, when a 14-electron metal fragment replaces a four-electron carbon, which could lead to new metallo-enediyne compounds for drug design.

CURRENT DEVELOPMENTS IN ENEDIYNE CHEMISTRY AND THE FUTURE

Enediynes had an important impact on organic chemistry. Today, one makes strategical use of the Bergman cyclization in organic synthesis.[20,21,30,31,51] To some extent, this holds also for the Meyers–Saito, Schmittel,[25,50] or the Garatt–Braveman reaction.[205] The Bergman cyclization had also its impact on the closely related Cope rearrangement.[13,206] The work on heteroenediynes and their nucleophilic cyclization

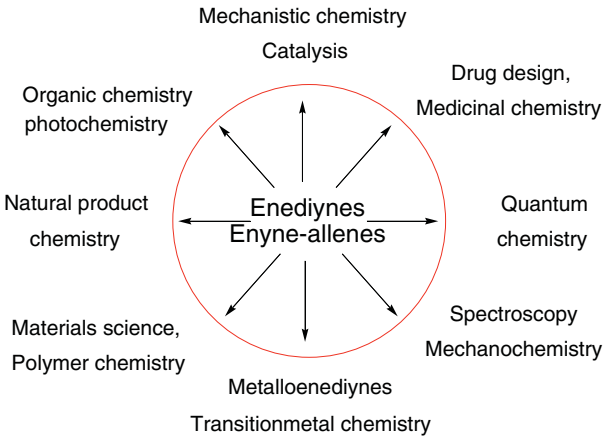

FIGURE 18 | The impact of enediynes and enyne-allenes on chemistry.

has turned out to be a promising method in heterocyclic synthesis.[31]

Interesting and relatively new are the studies on a photochemical triggering of the Bergman cyclization as, for example, in the case of the benzannulated cyclodeca-3,7-diene-1,5-diynes.[207] Based on these observations, Popik and co-workers[35] designed photoswitchable enediynes, which are stable in the dark, however undergo a cycloaromatization reaction to produce *p*-benzyne biradicals after irradiation with light of an appropriate wavelength. Alabugin and co-workers[208,209] recently designed hybrid molecules combining photoactivated aryl alkynes and a dicationic lysine moiety, which efficiently performs double-strand DNA cleavage. Catalyzed enediyne reactions[210–214] or reactions, in which the enediyne acts as a catalyst, e.g., for the synthesis of chiral products,[215] are also a novelty. Recently, enediynes have been used in gold chemistry for a new entry to domino reactions. Au attacks the triple bond to form a π-complex, which rearranges to form σ-bonded Au compounds. Hashmi and co-workers discovered that terminal 1,2-dialkynylarenes undergo an unexpected cyclization hydroarylation reaction toward naphthalene derivatives. The regioselectivity of the reaction can be controlled by tuning the gold catalyst.[214] Another peculiarity of enediyne chemistry is the (so far not successful) use of the enediyne core as a potentially useful mechanophore.[216]

Finally, it has to be mentioned that enediynes have found a special role in materials science and polymer chemistry.[217] Although still in its in infancy, the Bergman cyclization has already proven a valuable tool in polymer chemistry where it is applied in a twofold way: (i) The highly reactive *p*-benzynes generated by the Bergman cyclization can

© 2013 John Wiley & Sons, Ltd.

undergo polymerization acting either as monomers or initiators of other vinyl monomers thus leading to carbon-rich materials, e.g., glassycarbons and carbon nanotubes. In the case of homo-polymerization, high-density polymers with excellent thermochemical properties are obtained (see Figure 17(a)).[218] (ii) The Bergman cyclization can also be used to covalently modify carbon materials such as graphene (see Figure 17(b)), and in this way improve their poor solubility and dispersibility.[219]

In summary, the chemistry of enediynes has affected many fields of chemistry, for which Figure 18 provides an overview. There were times of enhanced and reduced interest in enediyne chemistry, and there were times where the work in this field was considered as superfluous. Even then, researchers from some times diametrically different fields in chemistry have proved these opinions as being wrong. In the year 2013, one can say that after more than 40 years, enediyne chemistry has still much to offer.

ACKNOWLEDGMENTS

This work was financially supported by the National Science Foundation, Grant CHE 1152357.

REFERENCES

1. Jones RR, Bergman RG. p-Benzyne. Generation as an intermediate in a thermal isomerization reaction and trapping evidence for the 1,4-benzenediyl structure. *J Am Chem Soc* 1972, 94:660–661.
2. Bergman RG. Reactive 1,4-dehydroaromatics. *Acc Chem Res* 1973, 6:25–31.
3. Darby N, Kim CU, Salaun JA, Shelton KW, Takada S, Masamune S. Concerning the 1,5-didehydro(10)annulene system. *J Chem Soc D* 1971, 1516–1517.
4. Edo K, Katamine S, Kitame F, Ishida N, Koide Y, Kusano G, Nozoe S. Naphthalenecarboxylic acid from neocarzinostatin (NCS). *J Antibiot* 1980, 33:347–351.
5. Lee MD, Dunne CT, Chang S, Ellestad GA, Siegel MM, Morton GO, McGahren WJ, Borders DB. Calichemicins, a novel family of antitumor antibiotics. 1. Chemistry and partial structure of calichemicin .gamma.1I. *J Am Chem Soc* 1987, 109:3466–3468.
6. Golik J, Clardy J, Dubay G, Groenewold G, Kawaguchi H, Konishi M, Krishnan B, Ohkuma H, Saitoh K, Doyle TW. Esperamicins, a novel class of potent antitumor antibiotics. 2. Structure of esperamicin X. *J Am Chem Soc* 1987, 109:3461–3462.
7. Konishi M, Ohkuma H, Matsumoto K, Tsuno T, Kamei H, Miyaki T, Oki T, Kawaguchi H, Vanduyne GD, Clardy. Dynemicin A, a novel antibiotic with the anthraquinone and 1,5-diyn-3-ene subunit. *J Antibiot* 1989, 42:1449–1452.
8. Meada H, Edo K, Ishida N. *The Past, Present, and Future of an Anticancer Drug*. New York: Mercell Dekker; 2003.
9. Ishida N, Miyazaki J, Kumagai K, Rikimaru M. Neocarzinostatin, an anti tumor antibiotic of high molecular weight. *J Antibiot (Tokyo) Ser A* 1965, 18:68–76.
10. Lüsers G, Köhnlein W, Jung G. Biological activity of the antitumor protein neocarzinostatin coupled to monoclonal antibody by *N*-succinimidyl 3-(2-pyridildithio) propionate (SPDP). *Biophys Struct Mech* 1981, 7:271.
11. Smith MB. *Organic Synthesis*. 3rd ed. New York: Academic Press; 2011.
12. Graulich N, Hopf H, Schreiner PR. Heuristic thinking makes a chemist smart. *Chem Soc Rev* 2010, 39:1503–1512.
13. Navarro-Vazquez A, Prall M, Schreiner PR. Cope reaction families: to be or not to be a biradical. *Org Lett* 2004, 6:2981–2984.
14. Mohamed RK, Peterson PW, Alabugin IV. Concerted reactions that produce diradicals and zwitterions: electronic, steric, conformational, and kinetic control of cycloaromatization processes. *Chem Rev* 2013, 113:7089–7129.
15. Raghavachari K, Trucks GW, Pople JA, Head-Gordon M. Fifth-order perturbation comparison of electron correlation theories. *Chem Phys Lett* 1989, 157:479–483.
16. Andersson K, Malmquist PA, Roos BO. Second-order perturbation theory with a complete active space self-consistent field reference function. *J Chem Phys* 1992, 96:1218–1226.
17. Parr RG, Yang W. *International Series of Monographs on Chemistry – 16. Density Functional Theory of Atoms and Molecules*. New York: Oxford University Press; 1989.

 © 2013 John Wiley & Sons, Ltd.

18. Border DB, Doyle TW. *Enediyne Antibiotics as Antitumor Agents*. New York: Springer; 1997.
19. Schreiner PR, Navarro-Vazquez A, Prall M. implicit and explicit coverage of multi-reference effects by density functional theory. *Acc Chem Res* 2005, 38:29–37.
20. Klein M, Walenzyk T, König B. Electronic effects on the Bergman cyclization of enediynes. A review. *Collect Czech Chem Commun* 2004, 69:945–965.
21. Gilmore K, Alabugin IV. Cyclizations of alkynes: revisiting BaldwinÕs rules for ring closure. *Chem Rev* 2011, 111:6513–6556.
22. Peterson PW, Mohamed RK, Alabugin IV. How to lose a bond in two ways - the diradical/zwitterion dichotomy in cycloaromatization reactions. *Eur J Org Chem* 2013, 2505–2527.
23. Wenthold PG. Thermochemical properties of the benzynes. *Australian J Chem* 2010, 63:1091–1098.
24. Wentrup C. The benzyne story. *Australian J Chem* 2010, 63:979–986.
25. Schmittel M, Vavilala C, Cinar EM. The thermal C2-C6 (Schmittel)/ene cyclization of enyne-allenes—crossing the boundary between classical and nonstatistical kinetics. *J Phys Org Chem* 2012, 25:182–197.
26. Sander W. *m*-Benzyne and *p*-benzyne. *Acc Chem Res* 1998, 32:669–676.
27. Alabugin IV, Yang WY, Pal R. Photochemical Bergman cyclization and related photoreactions of enediynes. In: Griesbeck A, Oelgemöller M, Ghetti F, eds. *CRC Handbook of Organic Photochemistry and Photobiology*. Boca Raton, FL: Taylor and Francis; 2012, 549–592.
28. Joshi MC, Rawat DS. Recent developments in enediyne chemistry. *Chem Biodiversity* 2012, 9:459–498.
29. Nicolaou KC, Chen JS. The art of total synthesis through cascade reactions. *Chem Soc Rev* 2009, 38:2103–2117.
30. Maretina IA. Design strategy of enediynes and enyne-allenes. *Russ J Gen Chem* 2008, 78:223–257.
31. Gulevskaya AV, Tyaglivy AS. Nucleophilic cyclization of enediynes as a method for polynuclear heterocycle synthesis. *Chem Heterolytic Compounds* 2012, 48:82–94.
32. Liang ZX. Complexity and simplicity in the biosynthesis of enediyne natural products. *Nat Prod Rep* 2010, 27:499–528.
33. Kar M, Basak A. Design, synthesis, and biological activity of unnatural enediynes and related analogues equipped with pH-dependent or phototriggering devices. *Chem Rev* 2007, 107:2861–2890.
34. Shao RG. Pharmacology and therapeutic applications of enediyne anti tumor antibiotics. *Curr Mol Pharmacol* 2008, 1:50–60.
35. Polukhtine A, Karpov G, Popik VV. Towards photoswitchable enediyne antibiotics: single and two-photon triggering of Bergman cyclization. *Curr Top Med Chem* 2008, 8:460–469.
36. Olano C, Mendez C, Salas JA. Antitumor compounds from marine actinomycetes. *Mar Drugs* 2009, 7:210–248.
37. Prall M, Wittkopp A, Schreiner PR. Can fulvenes form from enediynes? a systematic high-level computational study on parent and benzannelated enediyne and enyne-allene cyclizations. *J Phys Chem A* 2001, 105:9265–9274.
38. Vavilala C, Bryne N, Kraml C, Ho DM, Pascal JRA. Thermal C1-C5 diradical cyclization of enediynes. *J Am Chem Soc* 2008, 130:13549–13551.
39. Myers A, Kuo E, Finney N. Thermal generation of alpha,3-dehydrotoluene from (*Z*)-1,2,4-heptatrien-6-yne. *J Am Chem Soc* 1989, 111:8057–8059.
40. Saito K, Watanabe T, Takahashi K. (4+2)-Type cycloadditions of tropone and heptafulvene derivatives with a tautomeric mixture of cycloheptatrienylidene and cycloheptatetraene. *Chem Lett* 1989, 1989:2099–2102.
41. Schmittel M, Strittmatter M, Kiau S. Switching from the Myers reaction to a new thermal cyclization mode in enyne-allenes. *Tetrahedron Lett* 1995, 36:4975–4978.
42. Roth WR, Hopf H, Horn C. 1,3,5-Cyclohexatrien-1,4-diyl und 2,4-Cyclohexadien-1,4-diyl. *Chem Ber* 1994, 127:1765–1779.
43. Gräfenstein J, Hjerpe AM, Kraka E, Cremer D. An accurate description of the Bergman reaction using restricted and unrestricted DFT: stability test, spin density, and on-top pair density. *J Phys Chem A* 2000, 104:1748–1761.
44. Wenthold PG, Squires RR, Lineberger WC. Ultraviolet photoelectron spectroscopy of the *o*-, *m*-, and *p*-benzyne negative ions. electron affinities and singlet? Triplet splittings for *o*-, *m*-, and *p*-benzyne. *J Am Chem Soc* 1998, 120:5279–5290.
45. Marquardt R, Balster A, Sander W, Kraka E, Cremer D, Radziszewsk JG. *p*-Benzyne. *Angew Chem, Int Ed Engl* 1998, 37:955–958.
46. Marquardt R, Sander W, Kraka E. *m*-Benzyne. *Angew Chem, Int Ed Engl* 1996, 35:746–748.
47. Sander W, Exner M, Winkler M, Balster A, Hjerpe A, Kraka E, Cremer D. Vibrational spectrum of *m*-benzyne: a matrix isolation and computational study. *J Am Chem Soc* 2002, 124:4822–4831.
48. McMahon RJ, Halter RJ, Fimmen RL, Wilson RJ, Peebles SA, Kuczkowski RL, Stanton JF. Equilibrium structure of cis-Hex-3-ene-1,5-diyne and relevance to the Bergman cyclization. *J Am Chem Soc* 2000, 122:939–949.
49. Myers AG, Dragovich PS, Kuo EY. Studies on the thermal generation and reactivity of a class of

 © 2013 John Wiley & Sons, Ltd.

(σ, π)-1,4-biradicals. *J Am Chem Soc* 1992, 114:9369–9386.

50. Sakai S, Nishitani M. Theoretical studies on Myers–Saito and Schmittel cyclization mechanisms of hepta-1,2,4-triene-6-yne. *J Phys Chem A* 2010, 114:11807–11813.
51. Bhattacharyya S, Zaleski JM. Metalloenediynes: advances in the design of thermally and photochemically activated diradical formation for biomedical applications. *Curr Top Med Chem* 2004, 4:1637–1654.
52. Nicolaou KC, Zuccarello G, Ogawa Y, Schweiger EJ, Kumazawa T. Cyclic conjugated enediynes related to calicheamicins and esperamicins: calculations, synthesis, and properties. *J Am Chem Soc* 1988, 110:48664868.
53. Magnus P, Fortt S, Pitterna T, Snyder JP. Synthetic and mechanistic studies on esperamicin A1 and calichemicin .gamma.1. Molecular strain rather than .pi.-bond proximity determines the cycloaromatization rates of bicyclo(7.3.1)enediynes. *J Am Chem Soc* 1990, 112:4986–4987.
54. Snyder JP. Monocyclic enediyne collapse to 1,4-diyl biradicals: a pathway under strain control. *J Am Chem Soc* 1990, 112:5367–5369.
55. Nicolaou KC, Zuccarello G, Riemer C, Estevez VA, Dai WM. Design, synthesis, and study of simple monocyclic conjugated enediynes. the 10-membered ring enediyne moiety of the enediyne anticancer antibiotics. *J Am Chem Soc* 1992, 114:7360–7371.
56. Kraka E, Cremer D. CCSD(T) Investigation of the Bergman cyclization of enediyne. relative stability of *o*-, *m*-, and *p*-didehydrobenzene. *J Am Chem Soc* 1994, 116:4929–4936.
57. Alabugin IV, Manoharan M. Reactant destabilization in the Bergman cyclization and rational design of light-and pH-activated enediynes. *J Phys Chem A* 2003, 107:3363–3371.
58. Wong HNC, Sondheimer F. 5,12-Dihydro-6,11-didehydronaphthacene. A derivative of 1,4-didehydronaphthalene. *Tetrahedron Lett* 1980, 21:217–220.
59. Ahlström B, Kraka E, Cremer D. The Bergman reaction of dynemicin A - a quantum chemical investigation. *Chem Phys Lett* 2002, 361:129–135.
60. Basak A, Bag SS, Majumder PA, Das AK, Bertolasi V. Effect of remote trigonal carbons on the kinetics of Bergman cyclization: Synthesis and chemical reactivity of pyridazinedione-based enediynes. *J Org Chem* 2004, 69:6927–6930.
61. Nicolaou KC, Chen JS, Dalby SM. From nature to the laboratory and into the clinic. *Bioorg Med Chem* 2009, 17:2290–2303.
62. Smith AL, Nicolaou KC. The enediyne antibiotics. *J Med Chem* 1996, 39:2103–2117.
63. Jean M, Tomasi S, van de Weghe P. When the nine-membered enediynes play hide and seek. *Org Biomol Chem* 2012, 10:7453–7456.
64. Jones GB, Warner PM. Electronic control of the Bergman cyclization: the remarkable role of vinyl substitution. *J Am Chem Soc* 2001, 123:2134–2145.
65. Prall M, Wittkopp A, Fokin AA, Schreiner PR. Substituent effects on the Bergman cyclization of (*Z*)-1,5-hexadiyne-3-enes: a systematic computational study. *J Comput Chem* 2001, 13:1605–1614.
66. Alabugin IV, Manoharan M, Kovalenko SV. Tuning rate of the bergman cyclization of benzannelated enediynes with ortho substituents. *Org Lett* 2002, 4:1119–1122.
67. Samanta D, Cinar ME, Das K, Schmittel M. Nonstatistical dynamic effects in the thermal C2-C6 Diels–Alder cyclization of enyne-allenes. *J Org Chem* 2013, 78:1451–1462.
68. Alabugin IV, Manoharan M. Rehybridization as a general mechanism for maximizing chemical and supramolecular bonding and a driving force for chemical reactions. *J Comput Chem* 2007, 107:373–390.
69. Jones GB, Plourde IGW. Electronic control of the Bergman cycloaromatization: synthesis and chemistry of chloroenediynes. *Org Lett* 2000, 2:1757–1759.
70. Plourde IGW, Warner PM, Parrish DA, Jones GB. Halo-enediynes: probing the electronic and stereoelectronic contributions to the Bergman cycloaromatization. *J Org Chem* 2002, 67:5369–5374.
71. Roth WR, Hopf H, Wasser T, Zimmermann H, Werner C. 1,4-Didehydronaphthalin. *Liebigs Ann* 1996, 1996:1691–1695.
72. Spence JD, Rios AC, Frost CM, McCutcheon MA, Cox CD, Chavez S, Fernandez R, Gherman BF. Syntheses, thermal reactivities, and computational studies of aryl-fused quinoxalenediynes: effect of extended benzannelation on Bergman cyclization energetics. *J Org Chem* 2012, 77:10329–10339.
73. Zeidan TA, Manoharan M, Alabugin IV. Ortho effect in the Bergman cyclization: interception of *p*-benzyne intermediate by intramolecular hydrogen abstraction. *J Org Chem* 2006, 71:954–961.
74. Zeidan TA, Kovalenko SV, Manoharan M, Alabugin IV. Ortho effect in the Bergman cyclization: comparison of experimental approaches and dissection of cycloaromatization kinetics. *J Org Chem* 2006, 71:962–975.
75. Lin CF, Lo YH, Hsieh MC, Chen YH, Wang JJ, Wu MJ. Cytotoxicities, cell cycle and caspase evaluations of 1,6-diaryl-3(*Z*)-hexen-1,5-diynes, 2-(6-aryl-3(*Z*)- hexen-1,5-diynyl)anilines and their derivatives. *Bioorg Med Chem* 2005, 13:3565–3575.
76. Lo YH, Lin IL, Lin CF, Hsu CC, Yang SH, Lind SR, Wu MJ. Novel acyclic enediynes inhibit Cyclin A and CDC25C expression and induce apoptosis

 © 2013 John Wiley & Sons, Ltd.

phenomenon to show potent antitumor proliferation. *Bioorg Med Chem* 2007, 15:4528–4536.

77. Jeric I, Chen HM. A synthetic route to enediyne-bridged amino acids. *Tetrahedron Lett* 2007, 48:4687–4690.
78. Gredicak M, Matanovic I, Zimmermann B, Jeric I. Bergman cyclization of acyclic amino acid derived enediynes leads to the formation of 2,3-dihydrobenzo(*f*)isoindoles. *J Org Chem* 2010, 75:6219–6228.
79. Rawat DS, Zaleski JM. Syntheses and thermal reactivities of symmetrically and asymmetrically substituted acyclic enediynes: steric control of Bergman cyclization temperatures. *Chem Commun* 2000, 2493–2494.
80. Zhao Z, Peng Y, Dalley N, Cannon J, Peterson M. Bergman cycloaromatization of imidazole-fused enediynes: the remarkable effect of N-aryl substitution. *Tetrahedron Lett* 2004, 44:3621–3624.
81. Gräfenstein J, Kraka E, Filatov M, Cremer D. Can unrestricted density-functional theory describe open shell singlet biradicals? *Int J Mol Sci* 2002, 3:360–394.
82. Gräfenstein J, Cremer D. Density functional theory for open-shell singlet biradicals. *Chem Phys Lett* 1998, 292:593–602.
83. Filatov M, Shaik S. Spin-restricted density functional approach to the open-shell problem. *Chem Phys Lett* 1998, 288:689–697.
84. Filatov M, Shaik S. A spin-restricted ensemble-referenced Kohn—Sham method and its application to diradicaloid situations. *Chem Phys Lett* 1999, 304:429–437.
85. Filatov M, Shaik S. Artificial symmetry breaking in radicals is avoided by the use of the ensemble-referenced Kohn–Sham (REKS) method. *Chem Phys Lett* 2000, 332:409–419.
86. Gräfenstein J, Cremer D. The combination of density functional theory with multi-configuration methods - CAS-DFT. *Chem Phys Lett* 2000, 316:569–577.
87. Gräfenstein J, Cremer D. Can density functional theory describe multi-reference systems? Investigation of carbenes and organic biradicals? *Phys Chem Chem Phys* 2000, 2:2091–2103.
88. Gräfenstein J, Cremer D. Development of a CAS-DFT method accounting for non-dynamical and dynamical electron correlation in a balanced way. *Mol Phys* 2005, 103:279–308.
89. Cremer D. Density functional theory: coverage of dynamic and non-dynamic electron correlation effects. *Mol Phys* 2001, 99:1899–1940.
90. Perdew JP, Zunger A. Self-interaction correction to density-functional approximations for many-electron systems. *Phys Rev B* 1981, 23:5048–5079.
91. Gräfenstein J, Kraka E, Cremer D. The impact of the self-interaction error on the density functional theory description of dissociating radical cations: ionic and covalent dissociation limits. *J Chem Phys* 2004, 120:524–539.
92. Gräfenstein J, Cremer D. The self-interaction error and the description of non-dynamic electron correlation in density functional theory. *Theor Chem Acc* 2009, 123:171–182.
93. Polo V, Kraka E, Cremer D. Electron correlation and the self-interaction error of density functional theory. *Mol Phys* 2002, 100:1771–1790.
94. Polo V, Kraka E, Cremer D. Some thoughts about the stability and reliability of commonly used exchange-correlation functionals—coverage of dynamic and nondynamic correlation effects. *Theor Chem Acc* 2002, 107:291–303.
95. Polo V, Gräfenstein J, Kraka E, Cremer D. Influence of the self-interaction error on the structure of the DFT exchange hole. *Chem Phys Lett* 2002, 352:469–478.
96. Gräfenstein J, Kraka E, Cremer D. The impact of the self-interaction error on the density functional theory description of dissociating radical cations: Ionic and covalent dissociation limits. *Phys Chem Chem Phys* 2004, 6:1096–1112.
97. He Y, Gräfenstein J, Kraka E, Cremer D. What correlation effects are covered by density functional theory? *Mol Phys* 2000, 98:1639–1658.
98. Kraka E, Cremer D. Ortho-, meta-, and para-benzyne—a comparative CCSD(T) investigation. *Chem Phys Lett* 1993, 216:133–140.
99. Cremer D, Filatov M, Polo V, Kraka E, Shaik S. Implicit and explicit coverage of multi-reference effects by density functional theory. *Int J Mol Sci* 2002, 3:604–638.
100. Puiggros OR, Pittner J, Carsky P, Stampfuss P, Wenzel W. Multireference Brillouin-Wigner coupled cluster singles and doubles (MRBWCCSD) and multireference doubles configuration interaction (MRD-CI) calculations for the Bergman cyclization reaction. *Collect Czech Chem Commun* 2003, 68:2309–2321.
101. Lindh R, Persson BJ. Ab Initio Study of the Bergman reaction: the autoaromatization of hex-3-ene-1,5-diyne. *J Am Chem Soc* 1994, 116:4963–4969.
102. Hoffner J, Schottelius MJ, Feichtinger D, Chen P. Chemistry of the 2,5-didehydropyridine biradical: computational, kinetic, and trapping studies toward drug design. *J Am Chem Soc* 1998, 120:376–385.
103. Lindh R, Lee TJ, Bernhardsson A, Persson B, Karlström G. Extended ab initio and theoretical thermodynamics studies of the Bergman reaction and the energy splitting of the singlet *o*-, *m*-, and *p*-benzynes. *J Am Chem Soc* 1995, 117:7186–7194.
104. Dong H, Chen BZ, Huang MB, Lindh R. The Bergman cyclizations of the enediyne and its N-substituted analogs using multiconfigurational

 © 2013 John Wiley & Sons, Ltd.

second-order perturbation theory. *J Comput Chem* 2012, 33:537–549.

105. Seeger R, Pople JA. Self-consistent molecular orbital methods. XVIII. Constraints and stability in Hartree__ Fock theory. *J Chem Phys* 1977, 66:3045–3050.
106. Bauernschmitt R, Ahlrichs R. Stability analysis for solutions of the closed shell Kohn-Sham equation. *J Chem Phys* 1996, 104:9047–9052.
107. Lim MH, Worthington SE, Dulles FJ, Cramer C. Density-functional calculations of radicals and diradicals. In: Laird BB, Ross RB, Ziegler T, eds. *Chemical Applications of Density Functional Theory—ACS Symposium Series 629*. Washington, DC: American Chemical Society; 1996, 402–422.
108. Ziegler T, Rauk A, Baerends EJ. On the calculation of multiplet energies by the Hartree-Fock-Slater method. *J Theor Chim Acta* 1977, 43:261–271.
109. DeVisser SP, Filatov M, Shaik S. Myers–Saito and Schmittel cyclization of hepta-1,2,4-triene-6-yne: a theoretical REKS study. *Phys Chem Chem Phys* 2001, 3:1242–1245.
110. Chen WC, Zou JW, Yu CH. Density functional study of the ring effect on the Myers–Saito cyclization and a comparison with the Bergman cyclization. *J Org Chem* 2003, 68:3663–3672.
111. Engels B, Hanrath M. A theoretical comparison of two competing diradical cyclizations in enyne-allenes: the Myers—Saito and the novel C2-C6 cyclization. *J Am Chem Soc* 1998, 120:6356–6361.
112. Logan CF, Ma JC, Chen P. The photoelectron spectrum of the α,3-dehydrotoluene biradial. *J Am Chem Soc* 1994, 116:2137–2138.
113. Purvis GD III, Bartlett RJ. A full coupled-cluster singles and doubles model: the inclusion of disconnected triples. *J Chem Phys* 1982, 76:1910–1918.
114. He Z, Cremer D. Analysis of coupled cluster and quadratic configuration interaction theory in terms of sixth-order perturbation theory. *Int J Quant Chem* 1991, 25:43–70.
115. He Z, Cremer D. Analysis of coupled cluster methods. II. What is the best way to account for triple excitations in coupled cluster theory? *Theor Chim Acta* 1993, 85:305–323.
116. Crawford TD, Kraka E, Stanton JF, Cremer D. Problematic *p*-benzyne: orbital instabilities, biradical character, and broken symmetry. *J Chem Phys* 2001, 114:10638–10650.
117. Bersuker IB. *The Jahn-Teller Effect*. Cambridge: Cambridge University Press; 2006.
118. Crawford TD, Stanton JF, Allen WD, Schaefer HF. Hartree–Fock orbital instability envelopes in highly correlated single-reference wavefunctions. *J Chem Phys* 1997, 107:10626–10632.
119. Cremer D. Møller–Plesset perturbation theory. In: Schleyer PvR, Allinger NL, Clark T, Gasteiger J, Kollman PA, Schaefer HF, Schreiner PR, eds. *Encyclopedia of Computational Chemistry*, Volume 3. Chichester: John Wiley & Sons; 1998, 1706–1735.
120. Cremer D. Møller–Plesset perturbation theory, from small molecule methods to methods for thousand of atoms. *WIREs Comput Mol Sci* 2011, 509–530.
121. Brueckner KA. Nuclear saturation and two-body forces. II. Tensor forces. *Phys Rev* 1954, 96:508–516.
122. Handy NC, Pople JA, Head-Gordon M, Raghavachari K, Trucks GW. Size-consistent Brueckner theory limited to double substitutents. *Chem Phys Lett* 1989, 164:185–192.
123. Schreiner PR, Prall M. Myers–Saito versus C2-C6 (Schmittel) cyclizations of parent and monocyclic enyne-allenes: challenges to chemistry and computation. *J Am Chem Soc* 1999, 121:8615–8627.
124. Smith CE, Crawford TD, Cremer D. The structures of *m*-benzyne and tetrafluoro-*m*-benzyne. *J Chem Phys* 2005, 122:174309–174321.
125. Koga N, Morokuma K. Comparison of biradical formation between enediyne and enyne-allene. Ab initio CASSCF and MRSDCI study. *J Am Chem Soc* 1991, 113:1907–1911.
126. Andersson K, Malmqvist PA, Roos BO. Second-order perturbation theory with a complete active space self?consistent field reference function. *J Phys Chem* 1992, 96:1218–1226.
127. Carpenter BK. Electronically nonadiabatic thermal reactions of organic molecules. *Chem Soc Rev* 2006, 35:736–747.
128. Shavitt I, Bartlett RJ. *Many-Body Methods in Chemistry and Physics: MBPT and Coupled-Cluster Theory*. Cambridge: Cambridge University Press; 2009.
129. Evangelista FA, Allen WD, Schaefer HF. Comparison of biradical formation between enediyne and enyne-allene. ab initio CASSCF and MRSDCI study. *J Chem Phys* 2007, 127:1024102.
130. Li X, Paldus J. Multireference general-model-space state-universal and state-specific coupled-cluster approaches to excited states. *J Chem Phys* 2010, 133:184106.
131. Hanauer M, Köhn A. Pilot applications of internally contracted multi reference coupled cluster theory, and how to choose the cluster operator properly. *J Chem Phys* 2011, 134:204111.
132. Hamann PR, Upeslacis J, Borders DB. Enediynes. In: Cragg GM, Kingston GGI, Newman DJ, eds. *Anticancers Agents from Natural Products*. Boca Raton, FL: CRC Press; 2003, 575–621.
133. Edo K, Mizugaki M, Koide Y, Seto H, Furihata K, Otake N, Ishida N. The structure of neocarzinostatin chromophore possessing a novel bicyclo(7.3)dodecadiyne system. *Tetrahedron Lett* 1985, 26:33–340.
134. Konishi M, Ohkuma H, Saitoh K, Kawaguchi H, Golik J, Dubay G, Groenewold G, Krishnan B,

 © 2013 John Wiley & Sons, Ltd.

Doyle TW. Synthesis of the enediyne antibiotic esperamicin—a and novel analogues for tumor targeting. *J Antibiot* 1985, 38:1605–1609.

135. Clardy J, Walsh C. Lessons from natural molecules. *Nature* 2004, 432:479–483.
136. Gredicak M, Jeric I. Enediyne compounds—new promises in anticancer therapy. *Acta Pharm (Zagreb Croatica)* 2007, 57:133–150.
137. Ellestad GA. Structural and conformational features relevant to the anti-tumor activity of calicheamicin γ_1^I. *Chirality* 2011, 23:660–671.
138. Otani T, Minami Y, Sakawa K, Yoshida K. Isolation and characterization of non-protein chromophore and its degradation product from antibiotic C-1027. *J Antibiot* 1991, 44:566–568.
139. Komano K, Shimamura S, Norizuki D Yand Zhao, Kabuto C, Sato I, Hirama M. Total synthesis and structure revision of the maduropeptin chromophore. *J Am Chem Soc* 2009, 131:1207–12073.
140. Kawata S, Ashizawa S, Hirama M. Synthetic study of kedarcidin chromophore: revised structure. *J Am Chem Soc* 1997, 119:12012–12013.
141. Ando T, Ishii M, Kajiura T, Kameyama T, Miwa K, Sugiura Y. A new non-protein enediyne antibiotic N11999A2: unique enediyne chromophore similar to neocarzinostatin and DNA cleavage feature. *Tetrahedron Lett* 1998, 39:6495–6498.
142. Buchanan GO, Williams PG, Feling RH, Kauffman CA, Jensen PR, Fenical W. Sporolides A and B: structurally unprecedented halogenated macrolides from the marine actinomycete *Salinispora tropica*. *Org Lett* 2005, 7:2731–2734.
143. Oh D, Williams PG, Kauffman CA, Jensen PR, Fenical W. Cyanosporasides A and B, chloro- and cyano-cyclopenta (a) indene glycosides from the marine actinomycete *Salinisporapacifica*. *Org Lett* 2006, 8:1021–1024.
144. Lee MD, Dunne TS, Siegel MM, Chang CC, Morton GO, Borders DB. Calichemicins, a novel family of antitumor antibiotics. 1. chemistry and partial structure of calichemicin. gamma.1I. *J Am Chem Soc* 1987, 109:13464–3466.
145. Konishi M, Ohkuma H, Tsuno T, Oki T, Vanduyne GD, Clardy J. Crystal and molecular structure of dynemicin A: a novel 1,5-diyn-3-ene antitumor antibiotic. *J Am Chem Soc* 1990, 112:371–3716.
146. McDonald LA, Capson TL, Krishnamurthy G, Ding WD, Ellestad GA, Bernan VS, Maiese WM, Lassota P, Discafani C, Kramer RA, et al. Namenamicin, a new enediyne antitumor antibiotic from the marine ascidian *Polysyncraton lithostrotum*. *J Am Chem Soc* 1996, 118:10898–10899.
147. Oku N, Matsunaga S, Fusetani N. Shishijimicins A-C, novel enediyne antitumor antibiotics from the ascidian *Didemnum proliferum*. *J Am Chem Soc* 2003, 125:2044–2045.
148. Davies J, Wang H, Taylor T, Warabi K, Huang X, Andersen RJ. Uncialamycin, a new enediyne antibiotic. *Org Lett* 2005, 7:5233–5236.
149. Myers AG, Ling J, Hammond M, Harrington PM, Y W, Kuo E. Total synthesis of (+)-neocarzinostatin chromophore. *J Am Chem Soc* 1998, 120:5319–5320.
150. Inoue M, Ohashi I, Kawaguchi T, Hirama M. Total synthesis of the C-1027 chromophore core: extremely facile enediyne formation through SmI_2-mediated 1,2-elimination. *Angew Chem, Int Ed Engl* 2008, 47:1777–1779.
151. Schroeder DR, Colson KL, Klohr SE, Zein N, Langley DR, Lee MS, Matson JA, Doyle TW. Isolation, structure determination, and proposed mechanism of action for artifacts of maduropeptin chromophore. *J Am Chem Soc* 1994, 116:935–9352.
152. Ren F, Hogan PC, Anderson AJ, Myers AG. Kedarcidin chromophore-synthesis of its proposed structure and evidence for a stereochemical revision. *J Am Chem Soc* 2007, 129:12012–12013.
153. Ji N, ODowd H, Rosen BM, Myers AG. Enantioselective synthesis of N1999A2. *J Am Chem Soc* 2006, 128:14825–14827.
154. Nicolaou KC, Wang J, Tang Y, Botta L. Total synthesis of sporolide B and 9-epi-sporolide B. *J Am Chem Soc* 2010, 132:11350–11363.
155. Aburano D, Inagaki F, Tomonaga S, Mukai C. Synthesis of a core carbon framework of cyanosporasides A and B. *J Org Chem* 2009, 74:5590–5594.
156. Ulibani G, Audrain H, Nadler W, Lhermitte H, Grierson DS. Esperamicins, a novel class of potent antitumor antibiotics. I. Physico-chemical data and partial structure. *Pure Appl Chem* 1996, 68:601–604.
157. Nicolau KC, Hale CR, Nilewski C. A Total synthesis trilogy: calicheamicin gamma 1i, taxol, and brevetoxin A. *Chem Rec* 2012, 12:407–441.
158. Nicolaou KC, Hummel CW, Pitsinos EN, Nakada M, Smith AL, Shibayama K, Saimoto H. Total synthesis of calicheamicin gamma. 1I. *J Am Chem Soc* 1992, 114:10082–10084.
159. Hitchcock SA, Boyer SH, Chu-Moyer MY, Olson SH, Danishefsky SJ. A convergent total synthesis of calicheamicin gamma.1I. *Angew Chem Int Ed Engl* 1994, 33:858–862.
160. Shair MD, Yoon TY, Danishefsky SJ. Total synthesis of dynemicin A. *Angew Chem Int Ed Engl* 1995, 34:1721–1723.
161. Myers AG, Tom NJ, Fraley ME, Cohen SB, Madar DJ. A convergent synthetic route to (+)-dynemicin a and analogs of wide structural variability. *J Am Chem Soc* 1997, 119:6072–6094.
162. Weinstein DS, Nicolaou KC. Synthesis Of The namenamicin A-C disaccharide : towards the total synthesis of namenamicin. *J Chem Soc Perkin Trans I* 1999, 545–557.

 © 2013 John Wiley & Sons, Ltd.

163. Nicolaou KC, Kiappes L, Tian W, Gondi VB, Becker J. Synthesis of the carboline disaccharide domain of shishijimicin A. *Org Lett* 2012, 13:3924–3927.
164. Nicolaou KC, Zhang H, Chen JS, Crawford JJ, Pasunoori L. Total Synthesis and stereochemistry of uncialamycin. *Angew Chem Int Ed Engl* 2007, 46:470–4707.
165. Kobayashi S, Hirama M. Total synthesis of 9-membered enediyne antibiotic N1999-A2: absolute stereochemistry and DNA cleavage. *J Synth Org Chem Jpn* 2004, 62:184–193.
166. Nicolaou KC. Inspirations, discoveries, and future perspectives in total synthesis. *J Org Chem* 2008, 74:951–972.
167. Van Lanen SG, Shen B. Biosynthesis of enediyne antitumor antibiotics. *Curr Top Med Chem* 2008, 8:448–459.
168. Belecki K, Crawford JM, Townsend CA. Production of octaketide polyenes by the calicheamicin polyketide synthase CalE8: implications for the biosynthesis of enediyne core structures. *J Am Chem Soc* 2009, 131:12564–12566.
169. Belecki K, Crawford JM, Townsend CA. Deconstruction of iterative multidomainal polyketide synthase function. *Science* 2008, 320:243–246.
170. Crawford JM, Korman TP, Labonte JW, Vagstad AL, Hill EA, Kamari-Bidkorpeh O, Tsai SC, Townsend CA. Structural basis for biosynthetic programming of fungal aromatic polyketide cyclization. *Nature* 2009, 461:1139–1143.
171. Meunier B. *DNA and RNA Cleavers and Chemotherapy of Cancer and Viral Diseases*. NATO Science Series C. New York: Springer; 2010.
172. Tuesuwan B, Kerwin SM. 2-Alkynyl-*N*-propargyl pyridinium salts: pyridinium-based heterocyclic skipped-aza-enediynes that cleave DNA by deoxyribosyl hydrogen atom abstraction and guanine oxidation. *Biochemistry* 2006, 45:726–7276.
173. Tuttle T, Kraka E, Cremer D. Docking, Triggering and bioactivity of dynemicin A in DNA—a computational study. *J Am Chem Soc* 2005, 127:9469–9484.
174. Kraka E, Tuttle T, Cremer D. The reactivity of calicheamicin in the minor groove of DNA: the decisive role of the environment. *Chem Eur J* 2007, 13:9256–9269.
175. Tuttle T, Kraka E, Thiel W, Cremer D. A QM/MM study of the Bergman reaction of dynemicin A in the minor groove of DNA. *J Chem Phys B* 2007, 111:8321–8328.
176. Kraka E, Tuttle T, Cremer D. Design of a new warhead for the natural enediyne dynemicin A—an increase of biological activity. *J Chem Phys B* 2008, 112:2661–2670.
177. Zhao X, Wang S, Gao XF, Huang XR, Sun CC. Molecular dynamics simulations investigation of neocarzinostatin chromophore-releasing pathways from the holo-NCS protein. *J Struct Bio* 2010, 169: 14–24.
178. Goode JA, Chadwick DJ. *The Tumor Microenvironment: Causes and Consequences of Hypoxia and Acidity, Novartis Foundation Symposium 240*. New York: Wiley; 2009.
179. Toshima K, Ohta A, Ohashi A, Nakamura T, Nakata M, Tatsuta K, Matsumura S. Molecular design, chemical synthesis, and study of novel enediyne-sulfide systems related to the neocarzinostatin chromophore. *J Am Chem Soc* 1995, 117:4822–4831.
180. Suzuki I, Naoe Y, Bando M, Nemoto H, Shibuya M. pH Dependent cycloaromatization of enediyne model compounds via -oxo ketene acetal intermediates. *Tetrahedron Lett* 1998, 39:2361–2364.
181. Maji M, Mallick D, Mondal S, Anoop A, Bag SS, Basak A, Jemmis ED. Selectivity in Garratt—Braverman cyclization: an experimental and computational study. *Org Lett* 2011, 13:888–891.
182. Banfi L, Guanti G. Synthesis of a new lactenediyne scaffold equipped with three handles. *Tetrahedron Lett* 2002, 43:7427–7429.
183. Dai WM, Fong KC, Lau CW, Zhau L, Hamaguchi W, Nishimoto SI. Synthesis and DNA cleavage study of a 10-membered ring enediyne formed via allylic rearrangement. *J Org Chem* 1999, 64:682–683.
184. Takahasi T, Tanake H, Matsuda A, Yamada H, Matsumoto T, Sugiura Y. Synthesis of 10-membered masked oxaenediyne analogue of kedarcidin-chr. and C-1027-chr., and its DNA cleaving activity. *Tetrahedron Lett* 1996, 37:2433–2436.
185. Semmelhack MF, Gallagher JJ, Minami T, Date T. The enol-keto trigger in initiating arene diradical formation in calicheamicin/esperamicin analogs. *J Am Chem Soc* 1993, 115:11618–11619.
186. Sherer EC, Kirschner KN, Pickard FC IV, Rein C, Feldgus S, Shield GC. Eiffcient and accurate characterization of the Bergman cyclization for several enediynes including an expanded substructure of esperamicin A. *J Phys Chem B* 2008, 112:16917–16934.
187. Griffiths JR. Are cancer cells acidic? *Br J Cancer* 1991, 64:425–427.
188. Wike-Hooley JL, Haveman J, Reinhold JS. The relevance of tumor pH to the treatment of malignant disease. *Radiother Oncol* 1984, 2:343–366.
189. Kraka E, Cremer D. Computer design of anticancer drugs. a new enediyne warhead. *J Am Chem Soc* 2000, 122:8245–8264.
190. Kraka E, Cremer D. Structure and stability of enediynes containing heteroatoms—a quantum chemical investigation. *J Mol Struct THEOCHEM* 2000, 506:191–211.

 © 2013 John Wiley & Sons, Ltd.

191. Kraka E, Cremer D. The para-didehydropyridine, para-didehydropyridinium, and related biradicals - a contribution to the chemistry of enediyne antitumor drugs. *J Comput Chem* 2001, 22:216–229.
192. McCarty MF, Whitaker J. Manipulating tumor acidification as a cancer treatment strategy. *Altern Med Rev* 2010, 15:264–272.
193. Lee I, Glickson JD, Dewhirst MW, Leeper DB, Burd R, Poptani H, Nadal L, McKenna WG, Biaglow JE. Effect of mild hyperglycemia meta-iodobenzylguanidine on the radiation response of R3230 Ac tumors. *Adv Exp Med Biol* 2003, 530:177–186.
194. Ganapathy V, Thangaraju M, Gopal E, Martin PM, Itagaki S, Miyauchi S, Prasad PD. Sodium-coupled monocarboxylate transporters in normal tissues and in cancer. *AAPS J* 2008, 10:193–199.
195. Cramer CJ. Bergman, Aza-Bergman, and protonated aza-Bergman Cyclizations and intermediate 2,5-arynes: chemistry and challenges to computation. *J Am Chem Soc* 1998, 120:6261–6269.
196. Shulka PK, Mishra KPC. Hydrogen atom abstraction reactions of the sugar moiety of 2′-deoxyguanosine with an oh radical: a quantum chemical study. *Int J Quant Chem* 2011, 25:2160–2169.
197. Laroche C, Li J, Kerwin SM. Cytotoxic 1,2-dialkynylimidazole-based aza-enediynes: Aza-Bergman rearrangement rates do not predict cytotoxicity. *J Med Chem* 2011, 54:5059–5069.
198. Di L, Kerns EH. ADME properties of drugs. In: Tadhg PB, ed. *Wiley Encyclopedia of Chemical Biology*. New York: John Wiley & Sons; 2008, 1–8.
199. Lindahl SE, Park H, Pink M, Zaleski JM. Utilizing redox-mediated Bergman cyclization toward the development of dual-action metalloenediyne therapeutics. *J Am Chem Soc* 2012, 135:3826–3833.
200. Warner BP, Millar S, Brone RD, Buchwald SL. Controlled acceleration and inhibition of Bergman cyclization by metal chlorides. *Science* 1995, 269: 814–816.
201. Kraft BJ, Coalter NL, Nath M, Clark AE, Siedle AR, Huffman JC, Zaleski JM. Photothermally induced Bergman cyclization of metalloenediynes via near-infrared ligand-to-metal charge-transfer excitation. *Inorg. Chem.* 2003, 42:1663–1672.
202. Boerner LJK, Pink M, Park H, LeSueur A, Zaleski JM. Spin-state control of thermal and photochemical Bergman cyclization. *Chem Comm* 2013, 49:2145–2147.
203. Boerner LJK, Mazumder S, Pink M, Zaleski JM. Conformational and electronic consequences in crafting extended, π-conjugated, light-harvesting macrocycles. *Chem Eur J* 2011, 17:14539–14551.
204. Brzostowska EM, Hoffmann R, Parish CA. Tuning the Bergman cyclization by introduction of metal fragments at various positions of the enediyne. metalla-Bergman cyclizations. *J Am Chem Soc* 2007, 129:4401–4409.
205. Maji M, Mallick D, Mondal S, Anoop A, Bag SS, Basak A, Jemmis ED. Selectivity in Garratt–Braverman cyclization: an experimental and computational study. *Organic Lett* 2011, 13:1637–1654.
206. Graulich N. The Cope rearrangement—the first born of a great family. *WIREs Comput Mol Sci* 2011, 172–190.
207. Karpov GV, Popik VV. Triggering of the Bergman cyclization by photochemical ring contraction. facile cycloaromatization of benzannulated cyclodeca-3,7-diene-1,5-diynes. *J Am Chem Soc* 2007, 129:3792–3793.
208. Yang WY, Roy S, Phrathep B, Rengert Z, Kenworthy R, Zorio DAR, Alabugin IV. Engineering pH-gated transitions for selective and efficient double- strand dna photocleavage in hypoxic tumors. *J Med Chem* 2011, 54:8501–8516.
209. Breiner B, Kaya K, Roy S, Yang WY, Alabugin IV. Hybrids of amino acids and acetylenic DNA-photocleavers: optimising efficiency and selectivity for cancer phototherapy. *Org Biomol Chem* 2012, 10:3974–3987.
210. Shariar M, Sohel A, Liu RS. Carbocyclisation of alkynes with external nucleophiles catalysed by gold, platinum and other electrophilic metals. *Chem Rev* 2009, 38:2269–2281.
211. Hou Q, Zhang Z, Kong F, Wang S. Assembly of fused indenes via Au(I)-catalyzed C1-C5 cyclization of enediynes bearing an internal nucleophile. *Chem Commun* 2013, 7:695–697.
212. Wang Q, Aparaj S, Akmedov N, Petersen J, Shi X. Ambient Schmittel cyclization promoted by chemoselective triazole-gold catalyst. *Org Lett* 2012, 14:1334–1337.
213. Ye L, Wang Y, Aue L D Hand Zhang. Experimental and computational evidence for gold vinylidenes: generation from terminal alkynes via a bifurcation pathway and facile C-H Insertions. *J Am Chem Soc* 2012, 134:31–34.
214. Hashmi ASK, Braun I, Rudolph M, Rominger F. The role of gold acetylides as a selectivity trigger and the importance of gem-diaurated species in the gold-catalyzed hydroarylating-aromatization of arene-diynes. *Organometallics* 2012, 31:644–661.
215. Campolo D, Gaudel-Siri A, Mondal S, Siri D, Besson E, Vanthuyne N, Nechab M, Bertrand MP. Mechanistic investigation of enediyne-connected amino ester rearrangement. theoretical rationale for the exclusive preference for 1,6- or 1,5-hydrogen atom transfer depending on the substrate. a potential

 © 2013 John Wiley & Sons, Ltd.

route to chiral naphthoazepine s. *J Org Chem* 2012, 77:2773–2783.

216. Hickenboth CR, Rule JD, Moore JS. Preparation of enediyne-crosslined networks and their reactivity under thermal and mechanical conditions. *Tetrahedron* 2008, 64:8435–8448.
217. Xiao Y, Hu A. Bergman cyclization in polymer chemistry and material science. *Macromol Rapid Commun* 2011, 32:1688–1698.
218. Ma J, Ma X, Deng S, Hu A. Synthesis of dendronized polymers through Bergman cyclization of enediyne-containing Frechet-type dendrimers. *J Polym Sci Part A: Polym Chem* 2011, 49:1368–1375.
219. Ma X, Li F, Wang Y, Hu A. Functionalization of pristine grapheme with conjugated polymers through diradical addition and propagation. *Chem Asian J* 2012, 7:2547–2550.

 © 2013 John Wiley & Sons, Ltd.